2016

Deflector effects in fixed bed (biomass) combustors and non-combusting packed beds

Babak Rashidian
Edith Cowan University

Edith Cowan University

Copyright Warning

Deflector effects in fixed bed (biomass) combustors and non-combusting packed beds

by

Babak Rashidian

(MESc)

A Thesis with Publications presented to Edith Cowan University in fulfilment of the requirement for the degree of
Doctor of Philosophy

School Of Engineering
Edith Cowan University
Joondalup, WA 6027, Australia

December 13, 2016

Abstract

Combustion can be used to thermally process biomass fuels and yield both heat and power in a sustainable manner. At present, direct combustion of solid biomass is the primary approach for generating electricity and heat when these fuels are used at a commercial scale.

Deflectors have been used in the freeboard section of industrial combustors to reduce radiant heat loss through flue gases and for particle emissions abatement. Freeboard deflectors can also influence emissions and freeboard temperature distributions by changing the flow dynamics. Despite much research into laboratory scale biomass combustion and packed beds, there have been no systematic studies into the impact of deflectors (heat shields) on the axial and radial temperature profiles, test methodologies used or the emissions in laboratory scale fixed bed biomass combustors operated on pelletised fuels.

Through a combination of experiments and numerical simulations, this research has investigated such issues in both high temperature fixed bed biomass combustors as well as relatively lower temperature (non-combusting) packed beds subject to different heating modes.

Experiments have been carried out on a laboratory scale (continuous feed) fixed bed combustor featuring both primary air (supplied through the fuel bed) as well as secondary air (in the freeboard). A freeboard deflector was located at different axial locations during this testing. The aim was to characterize deflector effects on burning rate, temperature distribution (near-wall and near-centreline) and gaseous emissions (NO, CO, CO_2) over a range of primary and secondary air flow rates. A systematic method has been developed to establish the steady state time period during the combustion process. In this regard, detailed analyses on the time series of thermocouples, emissions and fuel mass conversion data have been performed. The proposed method is based on calculating the percentile mean deviation of temperature and NO/CO emissions data which can provide a more effective means of resolving the stand of the steady state operating, compared to only using the time evolution of these variables. In addition, the significance of the thermocouple radiative corrections (losses) and its effect on the accuracy of measured temperatures has been investigated.

The results concluded that NO, CO and CO_2 emissions are affected by the presence of a deflector in the mid-range of combustion stoichiometry (λ=0.439-0.509). However, deflector effects were found to be most prominent for NO and CO emissions by reducing and rising their levels, respectively. Deflectors affect upstream near-wall temperatures, but their impact depends on relative (axial) position (H). Furthermore, results reveal that deflectors do not have significant effects on the burning rate and flow availability of the exhaust gases.

A CFD model of a porous media has been implanted to study the effects of freeboard deflectors on the heat transfer inside packed bed columns for the temperature range of 100°C to 400°C (which is typical for drying and volatile release in biomass combustion). Results show that the deflector do affect temperature profiles along the freeboard as well as wall temperatures but this is dependent on the mode of heating and emissivity of the deflector.

Keywords: Experimental data, biomass combustion, freeboard deflector, CFD, temperature, emissions.

Declaration

I certify that this thesis does not, to the best of my knowledge and belief:

i. Incorporate without acknowledgement any material previously submitted for a degree or diploma in any institution of higher education;

ii. Contain any material previously published or written by another person except where due reference is made in the text; or Contain any defamatory material.

iii. I also grant permission for the Library at Edith Cowan University to make duplicate copies of my thesis as required.

Signed: Babak Rashidian

Data: 13/12/2016

Acknowledgements

My gratitude goes to a number of people, without whom it would have not been possible for me to undertake this program during my years at Edith Cowan University.

I sincerely thank my Principal Supervisor, Dr. Yasir Al-Abdeli, and Associate Supervisors, Prof. Guan Heng Yeoh, Dr. Ferdinando Guzzomi and for their invaluable time, continuous moral support, insightful guidance and constructive criticism since the start of the program. Dr Miccal Mathews is thankfully acknowledged for clarifying some fundamental aspects of modelling and experimental parts.

I greatly appreciate the support received through the collaborative work undertaken with the Energetic Technology Group (GTE) at University of Vigo, Spain. Special mention goes to Dr. David Patiño Vilas and Prof. Jacobo Porteiro for their invaluable support, scholarly comments and making those few months of data collection all the more interesting. To Ms. Araceli Regueiro Pereira for assisting with some aspects of the data acquisition undertaken by me at the University of Vigo and all the students and technical staff of the GTE group.

I am thankful to the technical and admin staff of the School of Engineering at ECU for their cooperation with regard to the project. The PhD research project is made possible by an Edith Cowan University International Postgraduate Research Scholarship (ECU-IPRS).

The anonymous reviewers of different internationally recognized journals and the thesis are also thanked for their precious time and scholarly comments which were helpful in further developing the manuscripts.

Thanks are also due to my family, without whom nothing (or not much) would have been possible. All the support they have provided me over the years was the greatest gift anyone has ever given me. Finally I would like to thank all my friends in Australia who have supported me over the last few years.

List of Journal Publications Arising from this Candidature

Published Journal Papers

- Rashidian, B., Al-Abdeli, Y.M., Yeoh, G.H. and Guzzomi, F.G., 2015. *Effect of freeboard deflectors on the temperature distribution in packed beds*. Applied Thermal Engineering, 89, pp.134-143. DOI:10.1016/j.applthermaleng.2015.05.045
- Rashidian, B., Al-Abdeli, Y.M., Patiño, D., Guzzomi, F.G. and Yeoh, G.H., 2016. *Effect of freeboard deflectors in the fixed bed combustion of biomass*. Applied Thermal Engineering, 103, pp.543-552. DOI:10.1016/j.applthermaleng.2016.04.140
- Rashidian, B., Al-Abdeli, Y.M., Yeoh, G.H., Patiño, D. and Guzzomi, F., 2017. *Methodologies for processing fixed bed combustor data*. Combustion Science and Technology, 189 (1), pp. 79-102. DOI:10.1080/00102202.2016.1193497

Journal Papers Under Review

- Rashidian, B. and Al-Abdeli, Y.M., 2016. *Effect of freeboard deflectors on the exergy in a fixed bed combustor*. Applied Thermal Engineering.

Table of Contents

List of Tables

List of Figures

List of Symbols, Nomenclature

A_p	volumetric particle surface area ($m^{-2}m^{-3}$)
Bi	Biot number (hL/k)
C_p	heat capacity ($Jkg^{-1}K^{-1}$)
C_2	inertial resistance factor (m^{-1})
$C_{1\varepsilon}$, $C_{2\varepsilon}$, C_μ	model constants
D_p	equivalent spherical diameter of the packing (m)
d_p	particle diameter (m)
d_t	column diameter (m)
d_{TC}	thermocouple diameter (m)
E_a	activation energy ($Jmol^{-1}$)
e_f	flow availability ($Wmol^{-1}$)
e^{tm}	is the specific thermomechanical exergy ($Wmol^{-1}$)
F_i	mass forces of component i ($Nm-^3$)
G	mass velocity of fluid, based on empty column ($kgm^{-2}s$)
GCV	Gross Calorific Value ($MJkg^{-1}$)
H	distance between deflector and top of the packed bed or
h	deflector thickness (mm)
I_b	black body radiation
I_λ	intensity of radiation at the wave length λ (Wm^{-2} $sr^{-1}\mu m^{-1}$)
k	thermal conductivity ($Wm^{-1}K^{-1}$)
k_c	Arhenius-type kinetic rate constant ($kgm^{-2}s^{-1}$atm-1)
k_d	mass transfer coefficient (ms^{-1})
k_f	fluid thermal conductivity ($Wm^{-1}K^{-1}$)
k_e	effective thermal conductivity ($Wm^{-1}K^{-1}$)
k_e^0	thermal conductivity at zero flow ($Wm^{-1}K^{-1}$)
k_s	solid thermal conductivity ($Wm^{-1}K^{-1}$)
L	Bed height (m)
M_t	Mach number
M_i	combustion measured variable
NCV	Net Calorific Value ($MJkg^{-1}$)
Nu	Nusselt number
p	static pressure (Pa)
Δp	pressure loss (Pa)
Pr	Prandtl number (=$C_p\mu/k$)
Pr_t	turbulent Prandtl number
Q_p	primary air (lit min^{-1})
Q_s	secondary air (lit min^{-1})
$q(\vec{r})$	radiative heat flux vector (Wm^{-1})
R	universal gas constant (8.3144621 $Jmol^{-1}K^{-1}$)
Re	Reynolds number
Re_p	Particle Reynolds number ($Re_p=\rho u d_p/\mu$)
$\vec{r}$	position vector (m)
r_{dry}	rate of drying ($kgm^{-3}s^-1$)
r_{pyr}	rate of pyrolysis ($kgm^{-3}s^-1$)
s	coordinate along the path of a radiation ray (m)
T	temperature at any axial or radial location (K)

T_b	indicated (or measured) bead temperature (K)
T_g	actual gas temperature (K)
T_{so}	outer shield temperature for sheathed aspirated probes (K)
T_w	wall temperature (K)
u	velocity (ms^{-1})
V_s	superficial velocity (ms^{-1})
x	mole fraction
Y	mass fraction
Greek	
α	packed bed permeability (m^2)
β	coefficient of thermal expansion
Γ	diffusion coefficient
ε	dissipation rate of kinetic turbulence energy (m^2s^{-3})
ε_b	void fraction (%)
ε_{bo}	bead emissivity
ε_g	emissivity of gas
ε_{so}	thermocouple sheath emissivity
κ	turbulent kinetic energy (m^2s^{-2})
λ	laminar thermal conductivity ($Wm^{-1}K^{-1}$)
$\lambda_{Primary}$	air to fuel equivalence ratio (based on the primary air flow rate)
λ_t	turbulent thermal conductivity ($Wm^{-1}K^{-1}$)
λ_{Total}	air to fuel equivalence ratio (based on the primary air flow rate)
μ	dynamic viscosity ($kgm^{-1}s^{-1}$)
μ_t	turbulent viscosity (Pa s)
υ	vector of interstitial velocity (ms^{-1})
ξ	wave length
ρ	density (kgm^{-3})
σ	Stefan-Bolzmanns constant ($5.67\times10^{-8}Wm^{-2}K^{-4}$)
σ_k, σ_ε	equivalent parameters for Prandtl number for k and ε
Φ	scattering phase function
Ω_i	solid angle (sr)

Chapter 1

General Introduction[1]

1.1 Biomass energy

Energy conversion is the capacity to change or transform energy from naturally occurring forms to forms that can be practically applied by humans. Bioenergy is a type of renewable energy that is produced from biomass. Biomass includes all materials that are directly or indirectly derived from photosynthesis reactions, for example wood-derived fuels, fuel crops, agricultural and agro-industrial by-products, and animal manure. Biofuels can be considered as a renewable source of energy if they are based on sustainable harvesting or production [1, 2].

The use of solid, liquid and gaseous biofuels has generated increased in interest in many parts of the world. There are various reasons for this, such as:

- *Environmental benefits:* such as reduction of greenhouse gas emissions, soil advancement and reduced acid rains;
- *Improvement in energy security and trade balance:* small changes in fossil fuels can have an enormous impact on the economy. One way to build economic security is to diversify energy suppliers by using renewable energy sources, such as biomass fuels;
- *Reducing waste disposal problems:* using by-products such as municipal waste and making better use of resources; and
- *Job creation*.

At present, forestry as well as agricultural and municipal residues are the main raw materials that are used for the generation of heat and electricity in biomass power plants. Figure 1.1 shows the contribution of bioenergy in the total world energy consumption.

[1] This thesis is presented and organised as "Thesis with publication" format.

Worldwide, there is a growth in the use of biofuels due to the increasing price of fossil fuels, environmental concerns and growing energy demand. It is estimated that by 2050 the world energy demand will increase to 600-1000 EJ[1] (from the 2008 value of about 500 EJ). Also, the amount of energy obtained via renewable energy will increase dramatically, and the future demand for bioenergy could be up to 250 EJ/yr [3].

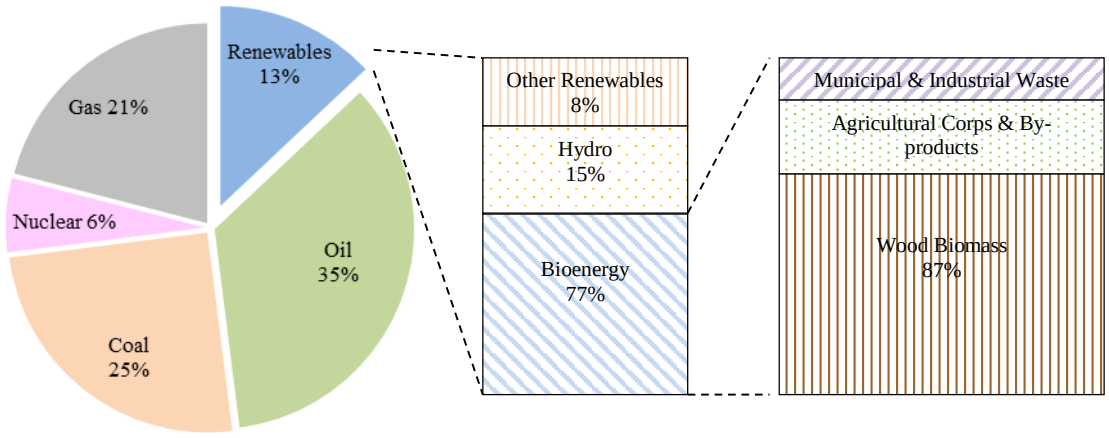

Figure 1.1 The contribution of bioenergy to world total energy consumption. Source: based on IEA[2], 2006; and IPCC[3], 2007 [3].

1.2 Biomass conversion technologies

There are three main methods to convert biomass into energy:

- *Thermal:* the most common way is to burn biomass to produce heat. This method can be used directly for heating and industrial processes, or indirectly to produce electricity. In industrial boilers, biomass is burned to produce high-pressure steam which can be used to generate electricity via turbines;
- *Thermochemical:* this method uses heat to break down biomass and process it into gas and liquid fuels such as methane and alcohol. Biomass reactors produce fuel gases (methane) by heating biomass in a low-oxygen

[1] 1 EJ = 10^{18} Joules (J)
[2] International Energy Agency
[3] Intergovernmental Panel on Climate Change

environment. Methane can fuel steam generators, fuel cells, turbines and combined cycle technologies; and

- *Biochemical:* this process uses bacteria, enzymes and yeast to ferment and convert biomass into alcohol (ethanol), which can be used directly (or mixed with standard gasoline) in vehicles. This process can also produce methane.

At present, the direct combustion of biomass is the primary approach for generating electricity and heat because it is cost competitive with fossil fuel alternatives. This method is often used in Combined Heat and Power (CHP) systems to improve efficiency. There are two main choices for the direct combustion of biomass; to burn the biomass on a grate (fixed or moving) or to fluidize the biomass with air or some other medium to provide. Figure 1.2 shows an overview of considered biofuels routes.

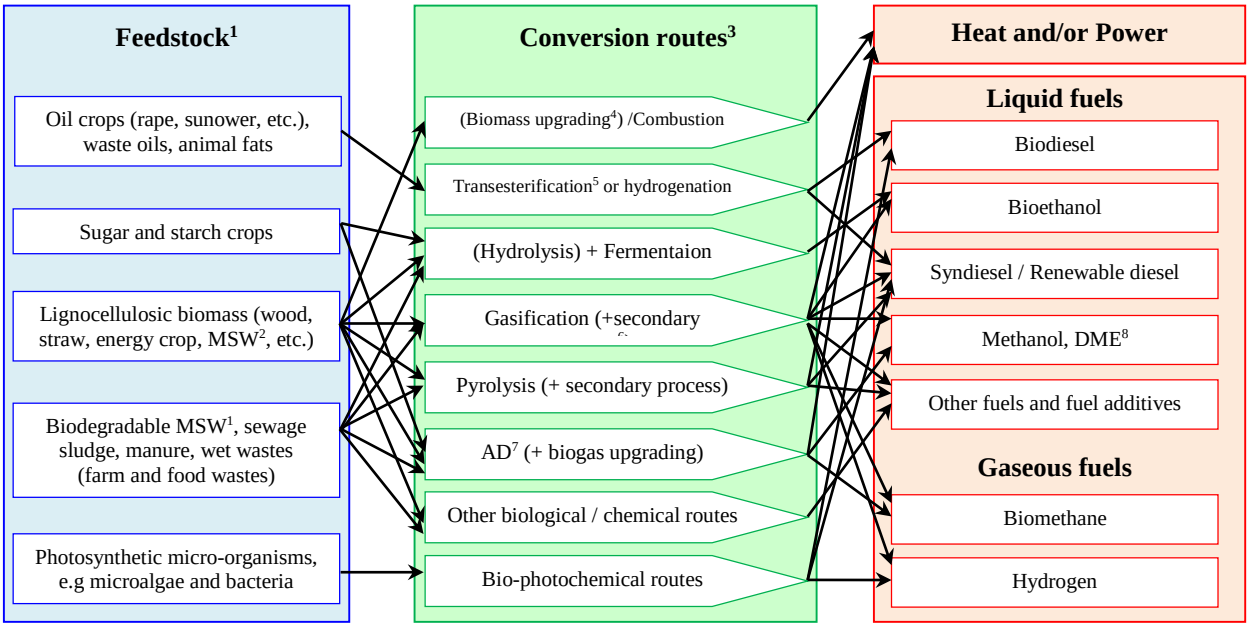

[1]Parts of each feedstock, e.g. crop residues, could also be used in other routes
[2] Municipal Solid Waste
[3]Each route also gives co-products
[4]Biomass upgrading includes any one of the densification processes (pelletisation, pyrolysis, torrefaction, etc.)
[5]Chemical conversion process that convert straight and waste vegetable oils into biodiesel
[6]Seperation processes, such as distillation
[7]AD = Anaerobic Digestion
[8]Dimethyl ether

Figure 1.2 Schematic view of the wide variety of bioenergy routes [4].

1.3 Biomass combustion process

The process of biomass combustion is very complex and consists of many physical and chemical aspects. Fuel properties and the combustion application are important

factors that affect the nature of the combustion process. The combustion process can be divided into a number of sub-processes: drying, pyrolysis, gasification and combustion. The time required for each process depends on the fuel size, fuel properties, temperature and combustion conditions. The combustion process can be continuous feed or batch, with air currents introduced being either forced or natural [6]. Figure 1.3 outlines the main stages and the temperature ranges associated with each stage.

The first steps in solid fuel combustion are drying and pyrolysis/gasification. The relative significance of these steps varies, depending on the combustion technology employed, the combustion process conditions, and fuel properties. In an industrial combustor with continuous feeding, such as moving grates, these processes will happen in different sections of the grate.

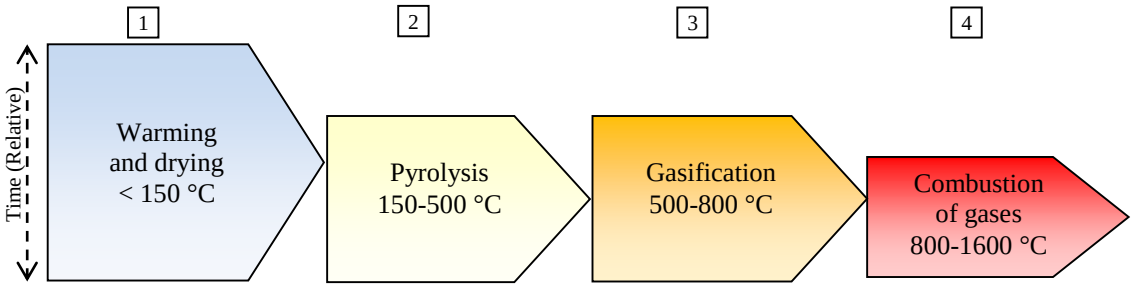

Figure 1.3 The four-stage combustion process (height of the pentagons show the relative time for each stage) [5].

Figure 1.4 shows the stages of burning for a small biomass particle. A brief overview of each stage is given in the literature [6].

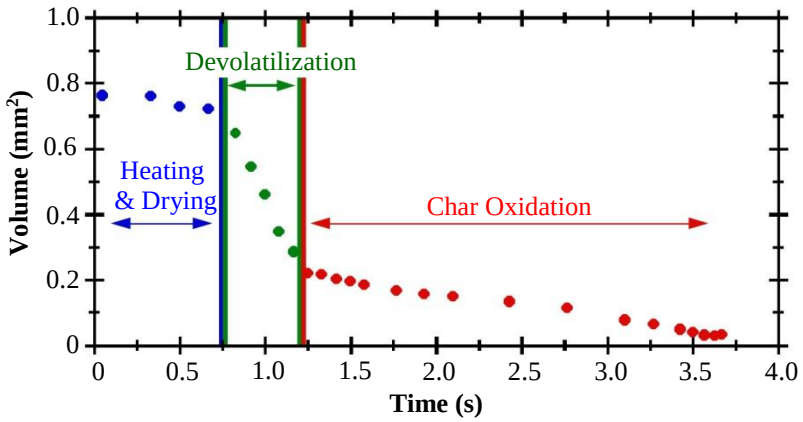

Figure 1.4 Stages of the burning process for a small biomass particle.

1.3.1 Drying

This stage involves evaporation of contained water. At low temperature (<100^{o}C) moisture starts to evaporate and vaporization lowers the temperature in the combustion chamber because it absorbs energy from the combustion process. Drying actively slows down the combustion process if the feed moisture content exceeds a certain amount, and the combustion process cannot continue (e. g., for wood) if the moisture content exceeds 60% on a wet basis [7]. Consequently, fuel moisture content is a very important variable whichever affect combustion performance.

1.3.2 Pyrolysis

Biomass is a fuel which consists of a high percentage of volatile matters as shown in Table 1.1 [8]. Pyrolysis is the thermal degradation (devolatilization) which takes place in the absence of an oxidizing agent, which decomposes fuel into volatile gases and solid char. Tar, charcoal, and low molecular weight gases are the primary products of pyrolysis. Since biomass is an oxygen-rich fuel, appreciable amounts of CO and CO_2 can be formed in this stage. The important process variables which affect the quantities and properties of the pyrolysis products are fuel type, pressure, reaction time and temperature.

Charcoal, and low molecular weight gases are the primary products of pyrolysis. Since biomass is an oxygen-rich fuel, appreciable amounts of CO and CO_2 can be formed in this stage. The important process variables which affect the quantities and properties of the pyrolysis products are fuel type, pressure, reaction time and temperature.

Table 1.1 Compositions for selected biomass fuels [8].

	Alfalfa stems	**Wheat straw**	**Rice hulls**	**Rice straw**	**Switch-grass**	**Sugar cane bagasse**	**Willow wood**	**Hybrid poplar**
Fixed carbon	15.81	17.71	16.22	15.86	14.34	11.95	16.07	12.49
Volatile matter	78.92	75.27	63.52	65.47	76.69	85.61	82.22	84.81
Ash	5.27	7.02	20.26	18.67	8.97	2.44	1.71	2.7

Proximate analysis (% dry fuel)

1.3.3 Gasification

Gasification is the thermal degradation (devolatilization) which takes place in the presence of an oxidizing agent. However, the term gasification is also used for char oxidation reactions. Gasification can be carried out with air, oxygen, steam or CO_2 as oxidizing agents. The main products of gasification are CO, CO_2, H_2O, H_2, CH_4 and other hydrocarbons.

1.3.4 Combustion

Complete oxidation of the fuel is defined as combustion. The hot flue gases that are produced through this stage can be used directly in boilers to generate steam for turbines. Biomass combustion processes take place in a homogenous-stage (volatile burning) and a heterogeneous-stage (coke combustion). According to the conditions of air supply and its mixture with the fuel, the velocity of the initial stage of combustion is generally higher than the velocity of the last stage when the fuel is burning in a solid state. In fixed bed grate combustion, the volatile matters are vaporized and burnt on the bed. The oxidizing air flows of the combustion can be categorised as either, the primary air which is used for the coke combustion, or the secondary air used for the volatile combustion [9].

Briefly, the combustion reaction of a fuel with air can be represented as follows:

$$\text{Biomass} + \text{Air} = \underbrace{CO_2 + SO_2 + H_2O}_{i} + \underbrace{N_2 + O_2}_{ii} + \underbrace{CO + H_2 + CH_4 + \text{soot}}_{iii} + \underbrace{\text{ash}}_{iv}$$

i) *Complete oxidation products:* CO_2 , SO_2 and H_2O. Sulfur content of biomass fuels is usually low so the percentage of SO_2 is almost insignificant.

ii) *Excess air* ($N_2 + O_2$) and, eventually, fuel and air moisture.

iii) *Gaseous products* (CO, H_2 and CH_4) and solid products from incomplete combustion (soot).

iv) *Biomass non-combustible mineral fraction* (ash).

Figure 1.5 shows the mass fraction of consumed fuel and the corresponding temperature of each stage for burning a single wood pellet [10].

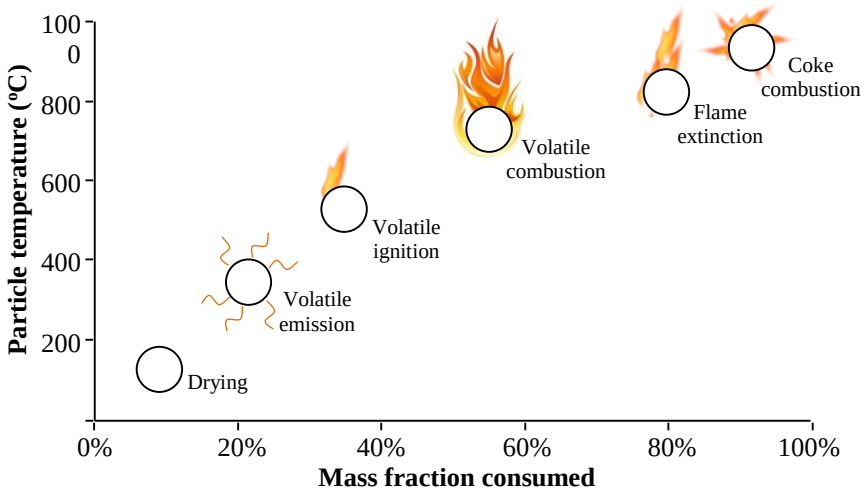

Figure 1.5 Wood pellet combustion stages.

1.4 Biomass fuels

Based on the types of pre-treatment undertaken of the raw fuel and fuel itself, biomass fuels can exist in a wide range of forms. The moisture content of those fuels may vary from 25 to 60 wt% (bark, sawmill side-products) or drop below 10 wt% (pellets, dry wood-processing residues). Pre-treatment technologies also affect the quality of the biomass fuels, so there is a trade-off between processed fuel cost ($/kg) and pre-treatment technology. Depending on the fuel preparation process, biomass fuels are available as bulk material (e.g. woodchips, sawdust) or unit material (e.g. straw bales, firewood) and the particle size distribution can be homogeneous (e.g. pellets) or inhomogeneous (e.g. untreated bark). Particle dimensions, bulk and energy density, gross and net calorific value and moisture content are important physical parameters [11].

The Gross Calorific Value (GCV), also known as the Higher Heating Value (HHV), is defined as the heat released during combustion per unit mass of fuel under the constraints that water formed during combustion is in a liquid phase and water and flue gas are returned to their initial temperature. The GCV of biomass fuels usually

varies between 18 and 22 MJ/kg and can be predicted from the ultimate analysis[1] according to the following empirical formula [12]:

$$GCV = 0.3491X_C + 1.1783X_H + 0.1005X_S - 0.0151X_N - 0.1034X_O - 0.0211X_{ash} \quad (1.1)$$

where X_i is the content of carbon (C), hydrogen (H), sulphur (S), nitrogen (N), oxygen (O) and ash in wt%.

The Net Calorific Value (NCV) also known as the Lower Heating Value (LHV), is defined as the heat released during combustion per unit mass of fuel under the constraints that the water formed during combustion is in a gaseous phase and that the water and the flue gas have the same temperature as the fuel prior to combustion. The NCV (MJ/kg) can be approximated as [12]:

$$NCV = GCV\left(1 - \frac{X_{mois}}{100}\right) - 2.444\frac{X_{mois}}{100} - 2.444 \times \frac{X_H}{100} \times 8.936\left(1 - \frac{X_{mois}}{100}\right) \quad (1.2)$$

where 2.444 is enthalpy difference between gaseous and liquid water at 25^{o}C, 8.936 is the ratio of the molecular weight of water to molecular weight of hydrogen (M_{H2O}/M_{H2}), X_{mois} is moisture content of the fuel in wt%, and X_H is the concentration of hydrogen in wt% . Table 1.2 shows GCV and NCV for selected biomass fuels and Figure 1.6 illustrates the heating values and change in the atomic ratios H/C and O/C from biomass composed of peat, lignite, coal and anthracite. The large H and O fractions result in large fractions of volatile species and a low char fraction compared to coal.

[1] Ultimate analysis is defined in ASTM D 3176 as the determination of the carbon and hydrogen in the material, as found in the gaseous products of its complete combustion, the determination of sulphur, nitrogen, and ash in the material as a whole, and the estimation of oxygen by difference.

Table 1.2 Moisture content, GCV, NCV, bulk density and energy density of biomass fuels [11].

	Moisture content (wt% w.b.)	**GCV** (MJ/kg d.b.)	**NCV** (MJ/kg d.b.)	**Bulk density** (kg w.b./m^3)	**Bulk energy** (MJ/m^3)
Wood pellets	10.0	19.8	16.4	600	9840
Woodchips-hardwood (pre-dried)	30.0	19.8	12.2	320	3900
Woodchips-hardwood	50.0	19.8	8.0	450	3600
Woodchips-softwood (pre-dried)	30.0	19.8	12.2	250	3050
Woodchips-softwood	50.0	19.8	8.0	350	2800
Grass (high-pressure bales)	18.0	18.4	13.7	200	2740
Bark	50.0	20.2	8.2	320	2620
Sawdust	50.0	19.8	8.0	240	1920
Straw (winter wheat)	15	18.7	14.5	120	1740

Abbreviations: GCV = gross calorific value; NCV = net calorific value; d.b. = dry basis; w.b. = wet basis.

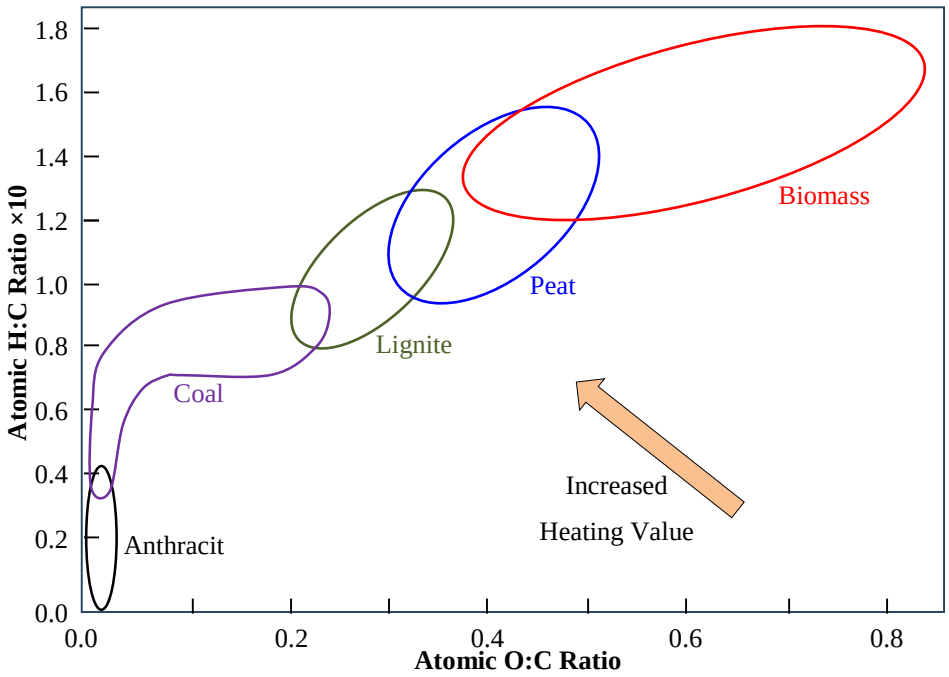

Figure 1.6 Atomic ratios H/C and O/C for solid fuels [13].

Table 1.3 shows some of the physical and chemical parameters of biomass fuels and their effects [11]. Table 1.4 shows some standards of the American Society for Testing and Materials (ASTM) for biomass fuels and Australian/New Zealand Standard standards for biomass fuels.

1.5 Biomass combustion technologies

Combustion is the most common way of converting biomass into heat which can be used to generate power if suitably integrated with boilers and prime movers like steam turbines. Over 90% of the energy generated from biomass worldwide is

provided by direct combustion, the simplest and most developed method compared to the other thermochemical technologies, such as wood-fired heating plants use for district heating and wood pellet burners [14]. Industrial combustion systems can be categorized as fixed bed combustion (FxBC), Fluidized Bed Combustion (FBC) and Dust Combustion (DC).

Table 1.3 The impact of various physical properties and chemical constituents on the behaviour of biomass fuels [11].

Physical properties	Effect
Moisture content	Storage durability and dry-matter losses, NCV, self-ignition, plant design
NCV, GCV	Fuel utilization, plant design
Volatiles	Thermal decomposition behaviour
Ash content	Dust emissions, ash manipulation, ash utilization/disposal, combustion technology
Ash-melting behaviour	Operational safety, combustion technology, process control system, hard deposit formation
Fungi	Health risks
Bulk density	Fuel logistics (storage, transport, handling)
Particle density	Thermal conductance, thermal decomposition
Physical dimension, form, size distribution	Hoisting and conveying, combustion technology, bridging, operational safety, drying, dust formation
Fine parts (wood pressings)	Storage volume, transport losses, dust formation
Abrasion resistance	Quality changes, segregation, fine parts
Chemical properties	
Carbon (C)	GCV
Hydrogen (H)	GCV, NCV
Oxygen (O)	GCV
Chlorine (Cl)	HCl, PCDD/PCDF emissions, corrosion, lowering ash-melting temperature
Nitrogen (N)	NOx, N_2O emissions
Sulphur (S)	SOx emissions, corrosion
Fluorine (F)	HF emissions, corrosion
Potassium (K)	Corrosion (heat exchangers, superheaters), lowering ash-melting temperature, aerosol formation, ash utilization (plant nutrient)
Sodium (Na)	Corrosion (heat exchangers, superheaters), lowering ash-melting temperature, aerosol formation
Magnesium (Mg)	Increase of ash-melting temperature, ash utilization (plant nutrient)
Calcium (Ca)	Increase of ash-melting temperature, ash utilization (plant nutrient)
Phosphorus (P)	Ash utilization (plant nutrient)
Heavy metals	Emissions, ash utilization, aerosol formation

Table 1.4 ASTM and Australian/New Zealand standards for biomass fuels.

ASTM No.	Description
ASTM E1690-08 [15]	Standard test method for determination of ethanol extractives in biomass
ASTM E1756 - 08 [16]	Standard test method for determination of total solids in biomass
ASTM E1721 - 01(2009) [17]	Standard test method for determination of acid-insoluble residue in biomass
ASTM E1758 - 01(2007) [18]	Standard test method for determination of carbohydrates in biomass by high performance liquid chromatography
ASTM E1755 - 01(2007) [19]	Standard test method for ash in biomass
ASTM E1757 - 01(2007) [20]	Standard practice for preparation of biomass for compositional analysis
ASTM E873 - 82 (2006) [21]	Standard test method for bulk density of densified particulate biomass fuels
ASTM E870 - 82 (2006) [22]	Standard test methods for analysis of wood fuels
ASTM E1534 - 93 (2006) [23]	Standard test method for determination of ash content of particulate wood fuels
AS/NZS No.	
4014.6 (2007) [24]	Domestic solid fuel burning appliances-Test fuels-Wood Pellets
5077 (2007)	Domestic solid fuel burning appliances-Pellet heaters-Determination of installation requirements and construction components
5078 (2007)	Domestic solid fuel burning appliances-Pellet heaters-Determination of power output and efficiency
4886 (2007)	Domestic solid fuel burning appliances-Pellet heaters-Determination of flue gas emission

1.5.1 Fixed bed combustion

Fixed bed combustion systems include grate furnaces and Underfeed Stokers. Figure 1.7 shows the different technologies for fixed bed combustion.

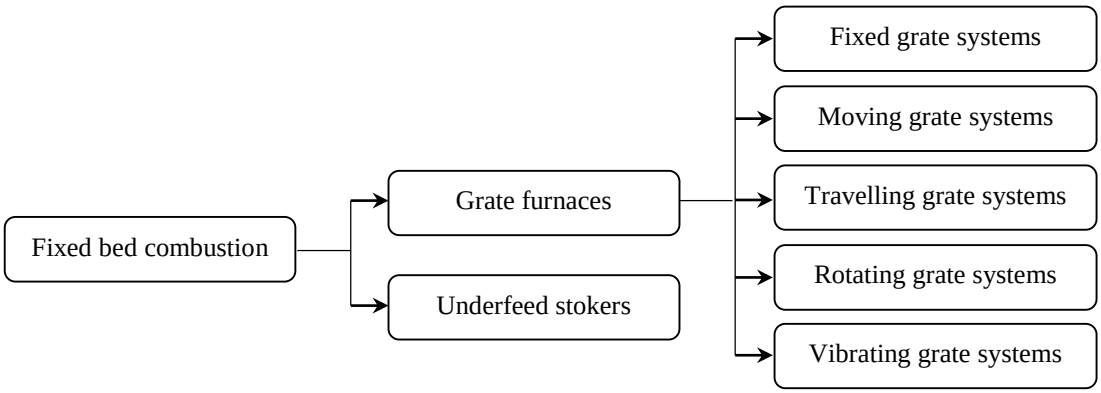

Figure 1.7 Fixed bed combustion technologies.

1.5.2 Fluidised bed combustion

Biomass fuel is burned in a self-mixing suspension of gas and solid-bed material while the air enters from beneath the reactor. To help fluidise the bed silica, sand and dolomite are common bed materials. A fluidised bed combustor is a cylindrical vessel with a perforated bottom plate filled with a suspension of inert materials. Because of the drastic heat transfer and mixing the complete combustion occurs with low excess air. Combustion temperature should be kept low (800-900°C) to prevent ash sintering in the bed. Fluidised bed combustors are flexible and can be fed with various fuels (e.g. mixture of straw and wood) due to good mixing in the bed. However fuel particle size and impurities are the main limitations of fluidised bed combustors [25]. Depending on the fluidisation velocity, fluidised beds can be divided into two categories; Bubbling Fluidised Beds (BFB) and Circulating Fluidised Beds (CFB).

In BFB furnaces, a bed material (such as silica sand of about 1.0 mm diameter) is located in the bottom part of the furnace with primary air is supplied over a nozzle distributor plate and fluidises the bed. The fluidisation velocity of the air varies between 1 and 3 m/s. To reduce NO_x emissions, secondary air is applied through several horizontally arranged nozzles at the beginning of the upper part of the furnace (called the freeboard) for enhancing staged-air supply. The advantage of BFB furnaces is their flexibility regarding particle size and moisture content of the biomass fuels. BFB are often proffered with fuels having low heat value and high moisture content. The big disadvantage of BFB furnaces is the operational difficulty at partial loads.

A circulating fluidised bed (CFB) operates at velocities between 3 and 10m/s and uses smaller sand particles (0.2 to 0.4mm in diameter) which are carried out with flue gases, but collected by cyclones, and fed back into the combustion chamber. The high turbulence in the combustion chamber makes for good mixing, very homogeneous temperature distribution in the bed and long residence time for fuel particles, providing good combustion and emission control. These combustors can utilize high heat value fuels with high moisture content. The disadvantages of CFB furnaces are their larger size, higher loss of bed material in the ash, and the small fuel particle sizes required. CFB furnaces are suitable for plants of more than

30MWth[1], due to their higher combustion efficiency and the lower flue gas flow produced [11].

1.5.3 Dust combustion (Pulverized combustion)

In dust combustors, fuels are injected and carried using air which also acts as an oxidiser. This type of combustor is suitable for small particles (average diameter less than 2mm). Fuel feeding should be carefully controlled because gasification of fine biomass particles produces an explosion-like environment. Fuel gasification and charcoal combustion occur at the same time because of the small particle size. Rotational flow is created by tangential injection of the fuel/air mixture. Fuel burns while it is in suspension, and gas burnout is achieved after secondary air addition. Dust combustors need low excess air amounts and emit low NO_x. However, complex feeding systems is the main downside [26].

Table 1.5 shows the combustion type and features of biomass fuels and Table 1.6 summarises advantages and disadvantages of the biomass combustion technologies.

Table 1.5 Combustion type and features of biomass [27].

Combustion method	Combustion type	Features
Fixed bed combustion	Horizontal/Inclined grate Watercooling grate Dumping grate	Grate is level or sloping. Ignites and burns as surface combustion of biomass supplied to grate. Used in small scale batch furnace for biomass containing little ash.
Moving bed combustion	Forward moving grate Reverse moving grate Step grate Louver grate	Grate moves gradually and is divided into combustion zone and after combustion zone. Due to continuous ash discharge, grate load is large. The combustion obstruction caused by ash can be avoided. Can be applied to wide range of fuels from chip type to block type.
Fluidized bed combustion	Bubbling fluidized bed combustion Circulation fluidized bed	Uses sand for bed material, keeps fuel and sand in furnace in boiling state with high-pressure combustion air, and burns through thermal storage and heat transmission effect of sand. Suitable for high moisture fuel or low grade fuel.
Rotary hearth combustion	Kiln furnace	Used for combustion of high moisture fuel such as liquid organic sludge and food residue, or large pieces etc. Restricted to fuel size.
Burner combustion	Burner	Burner burns wood powder and fine powder such as bagasse pith by burners, same as that for liquid fuel.

[1] Thermal power, MWth = approx 1000 kg steam/hour

1.6 Commercial scale systems

Underfeed Stoker: In Underfeed Stokers a screw conveyor is used to feed fuel into the combustion chamber from below. It is a cheap and operationally safe technology for small to medium scale systems up to a boiler capacity of 6MWth. Primary air is supplied through the grate, secondary air usually at the entrance to the secondary combustion chamber. Underfeed Stokers are appropriate for biomass fuels with low ash content (woodchips, sawdust, pellets) and particle sizes up to 50 mm. Biomass with high ash content (bark, straw and cereals) cause problems in underfeed stokers, as they clog the upper surface of the fuel bed due to sintered or melted ash. A simple loading systems is the main advantage of Underfeed Stokers because load changes can be achieved more easily and quickly than in grate combustion plants [11].

Moving Grate: The solid fuel is transported on a moving grate by alternating horizontal forward and backward motion. Primary air is supplied from below, and unburned and burned fuel particle are mixed. According to the different stages of combustion, the grate is divided into several parts, which can each be moved at various speeds [28].

Table 1.6 Advantages and disadvantages biomass combustion technologies.

Technology	Advantages	Disadvantages
Grate furnaces	○ low investment costs for plants < 20MWth ○ low operating costs ○ low dust emission ○ less sensitive to slagging	○ no mixing of fuels is possible ○ efficient NOx reduction requires special technologies ○ combustion conditions are not homogeneous
Underfeed stokers	• low investment costs for plants < 6MWth • simple load control • low emissions at partial load operation • high flexibility in regard to particle size	• suitable only for biomass fuels with low ash
BFB furnaces	○ no moving parts in the reactor ○ NOx reduction by air staging ○ high flexibility in moisture content and kind of biomass fuel ○ low excess air	○ high investment costs, interesting only for plants > 20MWth ○ high operating costs ○ low flexibility with regard to particle size ○ no utilization of high alkali biomass fuels ○ high dust load in the flue gas
CFB furnaces	• no moving parts in the reactor • NOx reduction by air staging • high flexibility in moisture content and kind of biomass fuel • very low excess air • homogeneous combustion • high specific heat transfer capacity due to high turbulence	• high investment costs, interesting only for plants > 30MWth • high operating costs • high sensitivity concerning ash slagging • no utilization of high alkali biomass fuels • high dust load in the flue gas
Pulverized fuel combustion	○ low excess air ○ high NOx reduction by efficient air staging ○ very good load control	○ particle size of biomass fuel is limited (< 10-20mm) ○ an extra start-up burner is necessary

Travelling Grate: The travelling grate is comprised of a chain that carries the pellets like a conveyor. The fuel bed itself does not move, but is transported through the combustion chamber by the grate. The primary air is used to cool the grate bar to prevent overheating. To achieve complete charcoal burnout, the speed of the travelling grate should continuously be controlled. A travelling grate system can provid uniform combustion conditions and low dust emissions. Also, the maintenance or replacement of a grate chain is relatively easy to handle. However the flow rate of the primary air is typically very high.

Rotating Grate: In a rotating grate combustor, conical grate sections rotate in opposite directions and are supplied with primary air from below. As a result, wet

and burning fuels are well mixed, which makes the system suitable for burning very wet fuels such as bark, sawdust and woodchips. Secondary air is applied in separate horizontal or vertical combustion chambers to help oxidise the combustion gases.

Vibrating Grate: The vibrating movement of the grate evenly distributes the fuel across the grate and primary air is applied from beneath. It is suitable for high ash fuels (e.g. straw, waste wood) which show sintering and slagging tendencies[1]. Disadvantages of vibrating grates are higher CO emissions, higher fly-ash emissions and controlling the fuel and ash transport [11, 29].

1.7 Small scale fixed bed systems

Fixed grate systems are only used in small scale applications. Such units are operated in houses or used for research purposes. According to the direction of the flame front propagation, there are two different types of bed configuration; counter-current and co-current. In the counter-current configuration, ignition starts at the top of bed and primary air is fed from beneath, while in a co-current configuration flame and primary air move upwards in the same direction. Fuel ignition and feed of primary air take place on the bottom bed. Figure 1.8 shows two different types of stationary bed systems, whilst Figure 1.9 shows the general bed structure and temperature profile in a fixed bed combustor [30]. This study will use a lab-scale fixed bed combustor in a counter-current configuration.

[1] Deposit formation on heat transfer surfaces of energy conversion equipment from the adhesion of sticky particles especially in zones closer to flame where the heat is mostly transferred by radiation.

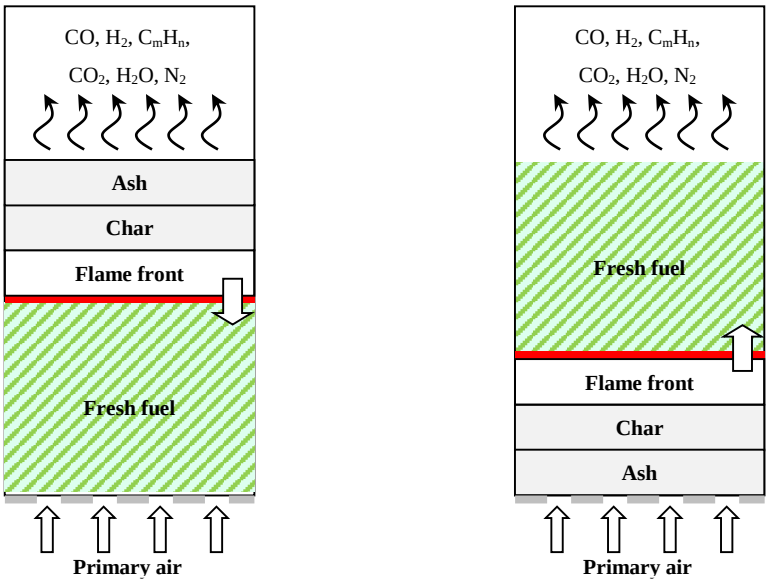

(a) Counter-current figuration (b) Co-current figuration

Figure 1.8 Thermal conversion in two different types of stationary bed configuration: (a) counter-current and (b) co-current conversion.

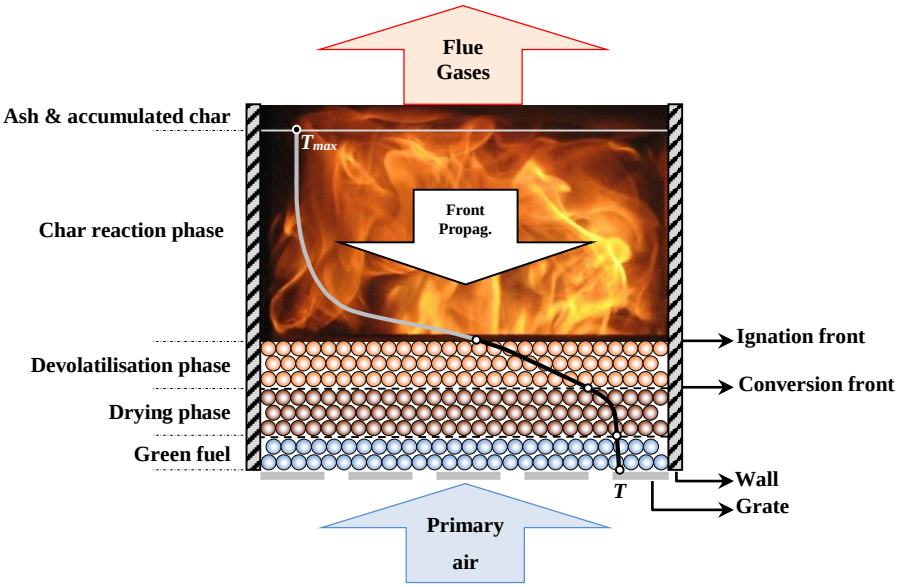

Figure 1.9 General bed structure and temperature profile in fixed bed combustor

The results of a fixed bed model can be applied to an industrial moving bed. Yang et al. [31] reported that a fixed bed reactor can be used to simulate the moving grate because the heat and mass transfer in the vertical direction is considered as the

dominating factor in a grate boiler. The results of the fixed bed model can be applied to an industrial moving bed. Figure 1.10 shows a schematic of a moving bed. The fuel migrates from left to right, and if the operating conditions do not change a pseudo-steady state will develop. Assuming that gradients in the x-direction are negligible, a transient 1-D model (in the z direction) can be used to simulate the whole fuel bed. If the migration velocity of the bed is known then it is possible to transfer time into the x direction of grate. This method has been widely used by different researchers to model moving beds [32].

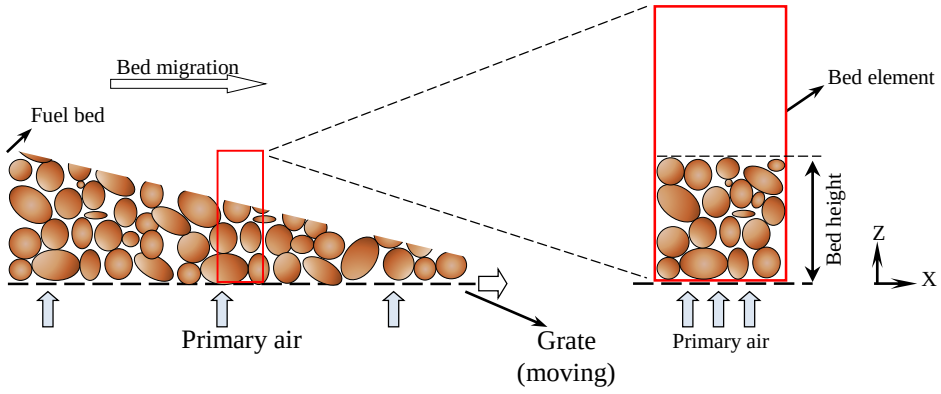

Figure 1.10 Simulation of moving bed furnace by fixed bed model.

1.8 Influential parameters in fixed bed combustion

Many parameters are known to affect the combustion process in the fixed bed reactors. According to their sources, these parameters can be categorized into three different groups which are shown in Table 1.7 [33]. Several experiments have been performed to investigate the parameters that influence the combustion of biomass in a laboratory scale fixed bed combustor. Air flow rate can be used to classify the combustion into three stages: oxygen limited, reaction limited and cooling by convection. In the oxygen limited regime, reactions are limited to surface reactions and velocity is controlled by the air supplied to the bed. In the reaction limited zone, the amount of oxygen is sufficient for oxidation and the overall reaction rate is controlled by the primary air velocity. By increasing the air flow rate the amount of excess air controls the reaction rate due to convective effects [34]. Figure 1.11 shows the behaviour of the fuel versus the air mass flow rate.

Table 1.7 The various influencing parameters on fixed bed combustion [33].

Fuel composition	Fuel morphology	Operating conditions
• Volatiles Content • Moisture Content • Ash Composition • Heating Value • Stoichiometric Air • Kinetic Constants • Specific Capacity • Thermal conduct. • Adiabatic Temp.	• Mean Particle Size • Mean Particle Shape • Particle Density • Bed Density • Porosity	• Thermal Effects • Total Air Supply • % Primary Air • % Secondary Air • Preheating • Insulation • Combustion Air Feeding Zone • Turbulence Generation

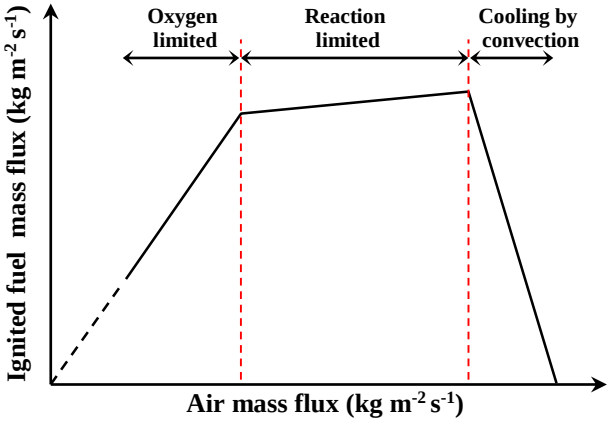

Figure 1.11 Three stages of the combustion according to the air flow rate [33].

Fuel moisture content also influences the performance, whereby decreasing the fuel moisture content increase both ignition[1] and the burning rate[2]. Fuel size is another parameter that affects the combustion process. Investigation of pellet fuels shows that the burning rate for small particles is higher compared to large particles [35]. However, particle size has no significant effect on the ignition speed [36]. The significance of thermal effects on these combustors is evident as using higher conductive materials will increase both the ignition and burning rates. Also, preheating the primary air accelerates the ignition and burning rates [35]. Insulation minimizes heat loss to the environment and increases the effect of drying and hence more heat is available inside the bed. Therefore, insulation boosts the ignition rate and burning rate [35].

[1] Ignition rate is defined as the speed of flame front propagation in the length of combustor (m/s).
[2] Burning rate is defined as kg ignited per cross section area and time (kg/m^{2}s).

1.9 Literature review

1.9.1 Thermal effects

Primary air: Preheating primary air has significant effects on the performance of biomass combustion by increasing the combustion chamber temperature significantly. The primary air temperature also has drying effects and has been studied by several authors [37-39]. More specifically, during a combustion reaction fuel particles undergo several processes. First, radiative heat from combustion at the top layer of a fuel bed can be absorbed by fuel particles as they are dried first. This heat absorbtion means less energy is available for fuel pyrolysis, which result in a lower ignition rate in the streamwise direction and a longer combustion time. Temporally, drying of fuel particles is then followed by a combination of pyrolysis and gasification. In these steps which follow an endothermic reaction, the fuel is decomposed and volatiles are rapidly emitted followed by partial oxidation. The final step, which again occurs at the bed surface, is complete oxidation, with char and carbon dioxide being the major products of this step [30].

The main effect of preheating is convective drying of the unignited bed [40]. Kessel et al. [37] reported the ignition rate also increases with primary air preheating. A similar result has been found by Gort [39] who concluded that when air preheating is used, the average ignition rate of the bed is higher than without preheating. Saastamoinen et al. [41] investigated the ignition front propagation in beds of wood particles both experimentally and theoretically and showed that air preheating increases the rate of flame propogation and combustion power. Moreover, air preheating also affects the emissions of biomass combustion. Doherty et al. [42] studied the effect of air preheating in a biomass gasifier and found that air preheating increases the gas heating value as well as H_2 and CO production. Research has also shown that preheating has little effect after a critical air temperature is exceeded. With this in mind, increased combustion air temperature results in elevated the adiabatic flame temperature [43]. Salzmann [44] investigated fuel staging for NO_x reduction in biomass combustion and report similar results. Wiinikka and Gebart [45] also showed that it is possible to control NO_x formation by air staging throughout the reaction zone.

Radiative effects and bed temperature: Radiation has a significant effect on heat transfer within a packed fuel bed and also combustion process in fixed bed combustors. Radiative heat transfer from the reaction zone and walls (above the bed) affect drying, pyrolysis, gasification and combustion of solid fuel particles in the fuel bed [46]. Radiative heat loss from the reaction zone can also diminish the reaction zone temperature, and as a result combustion performance will be decreased. Alternatively, if the temperature inside the bed increases, the ignition front propagates faster and causes solid fuel conversion rates to increase [35]. In industrial scale furnaces radiative effects are significant

The Radiation Transfer Equation (RTE) describes the radiative transfer process for an absorbing, emitting, and scattering medium [47]. The small fly-ash, soot and char particles have considerable effects on radiation heat transfer. Numerical calculations of their effects is complicated and time consuming, in particular when radiative properties and three-dimensional geometries are also considered [46]. Nilsson and Sunden [48] studied numerically radiation heat transfer in a simulated biomass combustor. They developed a new model for radiation heat transfer by using steady state, 2D and P_1[1] approximations to solve the RTE equation. In this regard the fixed bed was treated as a porous medium although bed radiation was taken into account, but their analysis did not consider radiation effects for other mediums inside the reactor nor were the prediction validated experimentally. Klason et al. [46] also investigated the radiative heat transfer process in two fixed bed biomass furnaces; a small scale (10kW) wood pellet furnace and a large scale (50MW) cross-current furnace and compared the simple Optically Thin (OT)[2] model, the spherical harmonic P_1-approximation model, and Spectral Line Weighted-sum-of-grey-gases model (SLW)[3]. They also observed that radiative heat transfer rates (to the fuel bed) are not very sensitive to the radiative properties of surfaces, but predictions are sensitive to the different radiative heat transfer models. They concluded that more computationally demanding models such as the SLW

[1] In an absorbing, emitting and scattering medium the radiative intensity can be expressed by a series spherical harmonics. The first term of the spherical harmonics series is the so-called P_1-approximation.
[2] In this model it is assumed that the medium is optically thin.
[3] It is a comprehensive approach to calculate the radiative transfer in non-grey and non homogeneous medium. In the SLW model the wave-length dependence of radiative transfer is taken into account.

model are more precise for the prediction of the radiative heat transfer rate to the fuel bed or to the walls.

Internal heat deflectors: Primary pollutants formed in biomass combustion are particulate matter species and gaseous emissions such as CO, HC, NO_X, SO_X, as well as volatile organic compounds (VOC). Polycyclic aromatic hydrocarbons (PAH) are also emitted during incomplete combustion [49, 50]. Most of the emitted particulate matter have an aerodynamic diameter smaller than 10μm [51], with particles smaller than 1 μm being called fine particles or combustion aerosols [52]. Particles are produced by two main process; incomplete combustion of fuel which produces organic carbon (OC); or the nucleation of inorganic species coupled with their failure to burn out later, producing black carbon (BC) or soot [53]. In commercial systems particle removal devices are applied before the flue gases are emitted through the stack into the atmosphere [54] and include [55]:

- Electrostatic precipitators (ESPS)
- Fabric filter systems
- Cyclones
- Afterburners
- Absorption & wet scrubbing equipment
- Deflectors

Lack of systematic understanding of the mechanisms by which deflectors affect both non-reacting packed beds and combusting packed beds, but it is speculated they have two effects. Firstly, it reduces particle emissions by decreasing the draft force of the flue gases which potentially increases residence time. Secondly, it enhances combustion performance by preventing flame radiation heat losses into the exhaust stack. Deflectors are widely used in industrial furnaces and boilers but little work has been done on them. Buczynski [56] investigated the use of deflectors in a counter-current fixed bed combustor, using both measurements and mathematical modelling, but the research was limited to coal fuel. A 3D model for time-dependent combustion was also developed to consider deflector effects and showed that deflectors can improve boiler operation based on repositioning the deflector, resulting in reduced emission of pollutants (CO, unburned hydrocarbons and fly ash). Most studies in the field of radiation modelling have not focussed on the simulation of a combustor with a heat shield.

Combustor wall and insulation: Heat is transferred by radiation, convection and conduction from the fuel bed to the combustor walls, as well as by conduction through the walls of the combustion chamber to the lower layers of fuel. The quantity of heat loss from the exterior shell of the combustor is the sum from convection and thermal radiation [57]. By improving combustion chamber insulation, these heat losses are minimised and a higher combustion chamber temperature can be achieved. An estimation of the amount of heat loss to the environment can be made by establishing an energy balance between the heat generated by combustion, heat taken up by flue gases and the heat transfered to the bed. Wiinikka and Gebart [58] reported that increasing the combustor wall temperature in a fixed bed wood pellet combustor yields a decrease in the emissions of coarse fly ash and soot particles; however, the emissions of submicrometer-sized fly ash particles simultaneously increase. However no attempt was undertaken to investigate the effects of the uniformity of temperature distribution across the bed on the accuracy of their numerical models.

Katunzi [59] investigated the effects of insulation in a fixed bed metal tube reactor and observed that heat lost from the reactor body decreases wall temperature and the speed of the reaction front. The ignition front propagation speed in an insulated combustor is also higher than in an un-insulated one because insulation prevents the heat loss to the environment and more heat is available for combustion and the bed temperature becomes higher which also affects fuel devolatilisation and drying. But there has been little work to describe the exact relationship between wall temperature and combustion performance. Buczynski [56] also described how different values of independent variables such as the amount of convective air, wall temperature or wall emissivity impact the mathematical modelling of combustion and defined a Logarithmic Sensitivity Factor (LSF)[1]. Sensitivity analysis revealed that model predictions were most sensitive to variations in excess air ratio[2], wall temperature and wall emissivity. Again no attempt was undertaken to establish the effects of heat loss from the combustor wall on the accuracy of the numerical model. Rogaume et al. [60] investigated the effects of different airflows (primary and

[1] A technique used to determine how different values of an independent variable will impact a particular dependent variable under a given set of assumptions.
[2] Excess air ratio= (Mass of air (kg) to combust one kg of fuel)/(Mass of stochiometric air)

secondary air) on the formation of pollutants during waste incineration and reported that by insulating the combustor wall radial heat losses are minimized and heat transfer along the reactor axis can be considered one dimensional. Yin et al. [61] also studied biomass combustion in an industrial 108MW grate-fired boiler both theoretically and experimentally, and found that deposits on the wall combustor act as insulation thereby affecting the combustion process. Katunzi [35] compared the burning rate of wood pellet fuel in glass, metal tube and insulated metal tube reactors and reported that with insulation on the reactor, the ignition speed and the burning rate are higher as compared to un-insulated and glass tube combustor. This phenomenon occurs because an insulated reactor wall transfers heat generated in the reaction zone to the fuel particles along the fuel bed, resulting in preheating of particles and easier ignition. Table 1.8 shows some important characteristics of combustors used in the literature [62]. In summary, although wall temperature is an important parameter which influences the combustion process, very little systematic work has been done into the effects of wall temperature and there is also ambiguity on the significance of boundary conditions (at the wall) on the accuracy and precision of numerical simulations in relation to fixed bed combustion.

1.9.2 Laboratory scale fixed bed combustor

Table 1.9 summarises the design parameters, thermocouples type and maximum reported temperatures of lab-scale test rigs addressed in the literature.

1.9.3 Mathematical modelling

To develop efficient biomass combustion technology it is necessary to understand the thermophysical mechanisms and process parameters which affect combustion. Various models have been developed during the last 50 years to simulate the combustion of biomass in packed beds. Although those research activities have ranged from simple models (with simplifying assumptions) to more complex methods (with a detailed description of the combustion reaction [63]), the level of assumptions employed generally affects the accuracy of outcomes. In this regard, packed bed models applicable to fixed bed combustion can be sorted either according to their level of approximation into homogenous, heterogenous, and pseudo-homogenous models (further described in [38]) or according to the solution method (analytical/numerical).

Table 1.8 Wall material and insulations of reactors used in the literature.

Principal Author	Cross-Section	Diameter (mm)	Height (mm)	Liner Material	Insulation
Nicholls [64]	circular	510	1120	Refractory lining	No insulation
Gort [39]	circular	300	800	Stainless steel	2 mm ceramic fibre (inside), 100 mm glass wool (outside)
Gort [39]	circular	200	800	Stainless steel	2 mm ceramic fibre (inside), 100 mm glass wool (outside)
Katunzi [35]	circular	56	500	Stainless steel	40 mm glass wool
Rogaume [60]	circular	200	2000	-[1]	40 mm refractory layer, 40 mm rock fiber (outside)
Wiinikka [58]	circular	200	1700	Stainless steel	The initial 600 mm of the cylindrical walls from the bottom of the reactor have been insulated
Van der Lans [65]	circular	150	1370	Stainless steel	-
Saastamoinen [41]	circular	224	300	-	-
Saastamoinen [41]	square	150 × 150	900	-	-
Samuelsson [66]	square	300 × 300	700	-	Well insulated
Weissinger [67]	circular	120	300	SiC[2]	Loose external, casing of firebrick
Yang [68]	circular	200	1500	Inconel[3]	Thick layer insulating material in tight casing
Ryu [69]	circular	100	1500	Inconel	80 mm insulation

[1] No data available
[2] Silicon carbide (SiC), also known as carborundum.
[3] A nickel-base alloy with chromium and iron.

Table 1.9 Main design parameters used for small scale fixed bed combustors.

Ref.	Combustor diameter (mm)	Combustor height (mm)	Fuel feed system	Type of thermocouples	Thermocouple diameter (mm)	No. of thermocouples	Max Temperature (ºC)	Thermocouples location
[69]	200	1500	Batch	K-type, S*	-	11	1200	-
[70]	200	1500	Batch	K-type, S*	-	11	800	-
[71]	154	1200	Batch	-	-	18	900	-
[72]	130	1050	Batch	K-type, S*	-	12	1000	-
[73]	230	-	Batch	B-type, BB▫	-	3	1500	-
[34]	150	1000	Batch	-	-	8	1200	-
[74]	180	1800	Batch	-	-	11	1000	-
[60]	200	2000	Batch	K-type, BB▫	0.5	28	1200	-
[35]	56	500	Batch	K-type, S*	-	7	1000	-
[37]	150	1500	Batch	-	-	6	900	-
[75]	200	600	Batch	K-type, S*	1, 2 and 3mm	2	1100	-
[41, 76]	150×150	900	Batch	-	-	3	1100	-
[77]	76×76	~440	Batch	B-type, S*	-	10	650	-
[78]	50	~1000	Batch	K-type, S*	-	8	1100	-
[79]	120×120	1500	Continuous	K-type, S*	-	1	1000	Freeboard
[80, 81]	20	1700	Continuous	S-type and N-type, BB▫	0.002	3	1400	Freeboard
[82]	100	2000	Continuous	K-type, S*	-	4	1000	Combustor wall
[83]	85	500-2500	Continuous	K-type	-	1	950	Freeboard
[84]	190	~3000	Continuous	R-type, S*	-	4	1350	Freeboard

*Sheathed thermocouple
▫Bare bead thermocouple

Models can also be classified according to the scale of modelling, whereby macroscale modelling indicates analysis which treats the bed as a whole, whilst microscale models will focous on a single porous fuel particle [62]. Sami et al. [85] presented a three mixture fractions/probability density function approach to simulate combustion for a blend of coal and manure in a swirl burner[1]. The development of CFD modelling for biomass combustion grew rapidly after this work.

Scharler et al. [86] used multi-step finite rate chemistry/eddy dissipation combustion model in the commercial software Fluent to simulate a grate boiler fired with waste wood and pellets. However, this model was not able to couple the heterogeneous biomass combustion on the grate and the turbulent reacting flow in the combustion chamber. Later, they developed their model by combining it with a finite cell based convective heat exchanger model [87].

[1] Swirl burner is one variation of Dust Combustion (DC) technologies. In the swirl system coal is injected through the centre of the burner with an annular swirling sawdust stream.

Yang et al. [68, 88] studied numerical models of biomass combustion as well as the effects of primary air in a packed bed boiler, and used a mathematical model to describe the phenomenon in the bed. Unlike Scharler, Yang avoided some complex factors such as a 3D temperature profile inside the particle and the mixing rate between the under-grate air and in this model. Later, they developed a numerical model for a full scale power plant furnace, assumed the bed cells were one of the three types (void cells, boundary cells and inner cells). They found that experimental results agree well with the predicted results [31, 89-91]. Ryu et al. [92] considered the k-ε turbulent model and expanded the application of this model to study the ignition and burning rates of segregated waste combustion. Yin et al. [61, 93-96] conducted modelling of an industrial boiler combustor and developed a CFD model for the biomass fired grate boiler, proposed two fuel bed models to couple with the CFD model, and evaluate the factors that may be important in modelling of biomass-fired grate boilers. Neither the Ryu nor the Yin did not consider the radiation effect of internal mediums in their models. Kaer et al. [97, 98] modelled the heat transfer inside the solid fuel bed by using a 1D bed model and showed that two combustion models existed in the bed; one characterized by a devolatilization front moving downwards, being followed by an upward moving char oxidization front; and another is that these two reactions both moves upwards. The first model was used to simulate the fuel bed and then the results were used as the inlet boundary conditions to calculate the turbulent combustion, which was modelled by the commercial CFD code CFX. However, they focused on predicting deposits (on the combustor walls) during the full scale boiler combustion and did not investigate the effect of deposits on the heat loss from the combustor walls.

Van der Lans et al. [65] developed a homogeneous 2D mathematical model for the combustion of straw in a grate furnace. Although, this model only considered the reactions of char with O_2, however the results still showed good agreement with the experimental data. Wei and Blasiak [99] performed modeling of an ecotube system[1] in coal and waste grate combustion, and assumed complex processes on the grate bed as homogeneous combustion of the gas phase in several well defined zones,

[1] The Ecotube-system is a new method for optimising the combustion process in boilers and furnaces by using retractable, water cooled nozzles. Various agents can be introduced through the nozzles at high pressure and velocity into the furnace media, resulting in destruction of laminar gas columns and the formation of completely mixed turbulent flow patterns.

and results show improvement in terms of boiler efficiency. Nevertheless, they did not simulate emissions of the CO_2 and corrosive chemicals such as SO_2 and H_2S in the flue gases. Zhou et al. [71] developed a 1D transient heterogeneous model for straw combustion in a fixed bed. Their simulation included evaporation, pyrolysis, heterogeneous reaction of char, and homogeneous reaction of volatiles and tar. They concluded that the effective heat conductivity, heat capacity of straw, and straw packing condition were the dominating factors influencing the combustion. They assumed fuel is composed of C, H as well as O and also did not consider the fragmentation, attrition or agglomeration of solids. Yu et al. [100] developed a model for the combustion of rice straw in a grate fired boiler under an air and oxygen rich operating condition and used FLIC (A Fluid Dynamic Incinerator Code) for the in-bed incineration and the commercial software FLUENT for the over-bed combustion. They showed that the combustion under the oxygen-enriched atmosphere accelerated combustion over conventional air. However, this model does not include the effect of internal heat deflector on the performance of combustion in the grate fired boiler. A summary of fix-bed combustion models and general governing equations are presented in Appendix C.

1.9.4 Performance of combustion

Four processes are often used to quantify the performance of combustion in fixed beds; the ignition front speed, burning rate, peak temperature and emissions.

Ignition speed: Ignition speed which is also referred as flame front speed or reaction front velocity is based on the temperature change along the bed [101]. It shows the distance travelled by the reaction front per unit time [35]. There are two procedures to calculate ignition rate:

- *Local ignition speed,* to calculate the ignition speed, time lag between two sequential thermocouples is divided by the distance between them.
- *Global ignition speed,* in this method the lag time between the first and last thermocouples is measured and divided by the distance between them (Figure 1.12) [35].

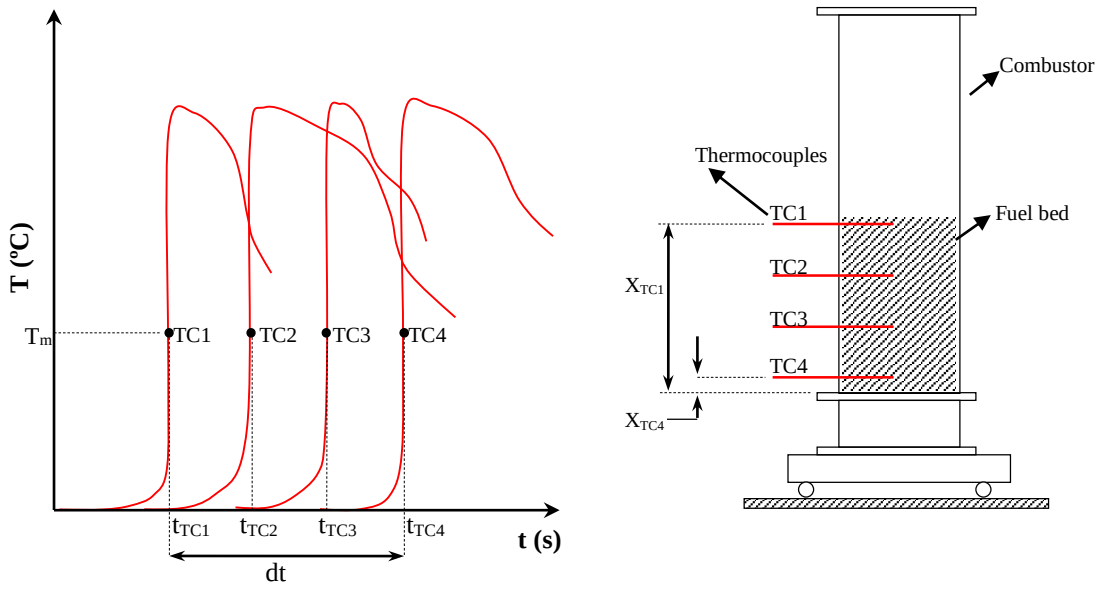

Figure 1.12 Determination of ignition speed.

Global ignition speed:

$$\bar{v}_f = \frac{X_{TC(1)} - X_{TC(N)}}{t_{TC(N)} - t_{TC(1)}} \tag{1.3}$$

Local ignition speed:

$$v_f = \frac{X_{TC(i)} - X_{TC(i+1)}}{t_{TC(i+1)}|_{T_m} - t_{TC(i)}|_{T_m}} \tag{1.4}$$

where v_f is the speed of the reaction front, x and t are position and time at the respective thermocouple.

Burning rate: The burning rate (ignition rate) is defined as the mass of fuel converted normalized to the combustor cross sectional and time (kg/m^{2}s) and expressed as:

$$\dot{m}_b = \frac{1}{A}\frac{dM}{dt} \tag{1.5}$$

In this regard, A is the cross section area of the fuel bed and *dM/dt* is the change in fuel mass per change in time [35] and includes raw (moist) fuel conversion into both char or gas. To calculate the fuel mass conversion, combustor mass can be monitored by a scale or weight mechanism. Figure 1.13 shows the procedure for determining the burning rate [35]. The fuel mass reduces as steps because of resolution of the weighting scales, so curve fitting can be performed.

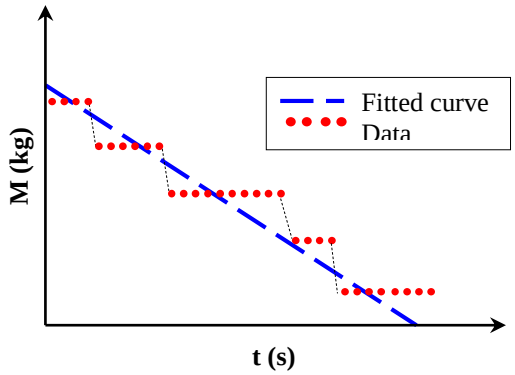

Figure 1.13 Burning rate calculation.

In the estimation of $\dot{m}_b$, only the fuel that is converted into gases is taken into consideration. If char formation occur, this is smaller than the amount of fuel ignited [62].

Peak temperature: The localised temperature has many effects on combustion processes such as drying pyrolysis and gasification [35]. The increase of the bed temperature results in an increase of fuel density, because chemical compounds with relatively low evaporation points, such as water and volatiles, are released to gas phase (vaporisation, devolatilization), leaving behind a solid phase which contains char and ash. Figure 1.14 shows a typical relationship between the wood pellet density and temperature. As such, the moisture content and solid fuel composition will vary continuously during combustion process as a function of bed temperature which also influences adiabatic combustion temperature.

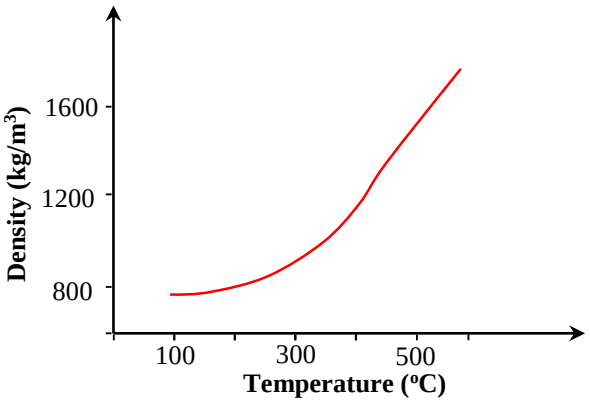

Figure 1.14 Variation of density with temperature.

Adiabatic combustion temperature increases as a function of degree of burnout[1] at a constant excess air ratio[2] [56]. Also the peak temperature is required for estimation of activation energy. In practice, the recorded temperature is fluctuated, because of particle movement in the bed. In this case the sum of the peak temperatures recorded at each thermocouple is taken and average value is calculated by dividing the sum of the peak temperatures to the number of thermocouples.

Emissions: Biomass is the most difficult to burn of the commonly used heating fuels. The amount of pollutants emitted to the atmosphere from different types of biomass combustion are highly dependent on the combustion technology implemented, the fuel properties and the combustion process conditions [102]. The amount of emissions released is one of the most important performance indicators in the biomass combustion. In this research project, the main focus on emissions is on CO, CO_2, NO_x. Many variables directly or indirectly influence emission levels such as bed temperature [35], fuel properties [68, 69], air distribution rate and secondary air [45]. Primary pollutants from biomass combustion can be classified into two groups: from incomplete combustion or from inorganic components in biofuels [95]. In counter-current combustion, three different regimes are identified oxygen-limited, reaction-limited and quenching by convection [103]. The emissions in these three zones is different, for example in char gasification zone in a reactor (0.2m in inner diameter and 2.0m in total height) under certain operating condition CO concentration increase from 15 (vol%) to 25 (vol%) and then decrease to 0 (vol%) [104].

1.10 Project motivation

Deflectors, which form the research focus of this project, are common in industrial combustors and have been extensively employed to improve combustion performance and decrease particle emission [105]. However, far less attention has been paid to investigate the effects of deflectors on biomass combustion in fixed beds reactors or the thermal effects in (non-reacting) packed beds. Even so, whilst few systematic researches into the effects of freeboard deflectors have been made, published studies [56, 106, 107] indicate that deflectors influence combustion

[1] The degree of oxidation in a combustion reaction
[2] Excess air ratio= (Mass of air (kg) to combust one kg of fuel)/(Stochiometric air)

performance by affecting the heat transfer and flow dynamics in the freeboard section. Since there are many similarities between fixed bed configurations and industrial systems where heat and mass transfer in the vertical direction is the dominating factor, small scale combustors have been used to study fundamental behaviour and performance in industrial moving grate combustors factor [31, 35, 63, 108]. As a result, there is a need to investigate the effects of deflectors on the temperature profiles, emissions and flue gas availability in laboratory scale fixed bed biomass combustor.

The key benefit of packed beds is the high surface area to volume ratio which suitable them for a wide range of engineering applications from chemical reactors [109-113] and fixed bed combustors [33, 114-116] to heat storage systems [117-119] and heat exchangers [120, 121]. Since (non-reacting) packed beds can also be used as a first step in studying the thermal performance in fixed bed combustors, the need to study these is also warranted. In counter-current fixed bed combustion biomass fuels are first heated up by initial ignition started from top of the bed and propagates downwards. Biomass usually contains moisture (which is stored in material structure) and volatile matter (typically from 10% to 70% of the original fuel mass) [88, 103]. In combusting packed beds heat transfer rates inside packed beds limit evaporation rates and other sub-processes such as volatile release rates [122]. Numerous numerical studies described the heat transfer and flow characterisation in non-combusting packed beds [109, 123-128]. Meanwhile, several unresolved problems persist. Such problems include the effects of porosity, wall temperature and fluid velocity on the effective thermal conductivity and temperature distributions in packed beds. Heat transfer relationships have been thoroughly studied both experimentally and theoretically but the derived equations are limited to low Reynolds numbers [129-131], non-drying particles [109] and deficient defined boundary condition [124, 132]. In Addition, the effect of freeboard deflectors on the axial pressure drop and temperature distribution have not been reported in the literature. This research have been investigated the effects of a deflector above a packed bed by using a of a three-dimensional Computational Fluid Dynamics (CFD) model of a porous media. The impact of freeboard deflectors on the pressure drop, axial and radial temperature profiles have been

studied for the temperature range of 100°C to 400°C which is typical for drying and volatile release in biomass combustion.

Thermal conversion processes are very sensitive to various parameters such as fuel characterizations, uniformity of fuel bed and fluctuation of primary and secondary air flowrates. Hence, extracting the steady state time period can be problematic by the time progression and variability of different test variables. Despite most researchers have been reported results derived from steady state operating behaviour, little detail has been published on systematic approaches to define the steady state testing regime [33, 35, 37, 102, 133-135]. In the absence of systematic method to discerning the steady state time period, there is an ambiguity in relation to how emissions, temperature and burning rate have been derived and presented. This research has addresses the above knowledge gaps by detailed analyses on the time series of thermocouples, emissions and fuel mass conversion data and developing a methodology to establish the onset of the steady state condition in fixed bed combustion.

Sheathed thermocouples are widely used for measuring temperatures inside the combustors. Temperature readings using such a device may significantly affected by radiative exchange errors [136]. Ignoring the radiative cooling effects of combustor walls may lead to remarkable errors in measured temperatures [137]. The significance of radiation losses depends on several parameters such as thermocouple sheath/bead emissivity, the flue gas properties (temperature, soot loading), thermocouple size, the surroundings temperature (combustor walls) and convective heat transfer in the vicinity of the thermocouple sheath/bead [138, 139]. Sheathed thermocouples offer higher reliability and reduce radiation errors [139, 140]. However, despite wide use of such thermocouples, there is a paucity of literature investigating the use or impact of any radiation corrections. Bridging this gap is one of the outcomes of this research.

1.11 Research questions

The overview above identifies existing challenges and unresolved issues in relation to freeboard deflectors and their effects on the performance of both non-reacting packed beds and fixed bed combustors. The research questions addressed in this doctoral thesis are briefly described below.

RQ1 In fixed bed combustors, what is the most effective method of ascertaining the steady state time period, both with and without freeboard deflectors? This research question will be addressed in Chapter 2.

RQ2 In fixed bed combustors, does the use of freebaord deflectors introduce any thermal effects which affect the method used to process thermocouple data, and if so, what is the order of these effects? This research question will be addressed in Chapter 2.

RQ3 For biomass combustion in fixed bed combustors, how does the axial location of an internal heat deflector affect the emissions, temperatures and fuel burning rate? This research question will be addressed in Chapter 3.

RQ4 In fixed bed combustors, what impact do freeboard deflectors have on the flue gases availability (exergy analyses)? This research question will be addressed in Chapter 4.

RQ5 In non-reactive packed beds, what effects do freeboard deflectors have on the temperatures and pressure drops inside the bed and above it (in the freebaord) and how does this vary with the mode of heating? This research question will be addressed in Chapter 5.

1.12 Research methodologies

The above research questions are addressed in this thesis by applying both experimental and numerical methodologies. The experimental methods include temperature, continuous emissions measurements and weight loss monitoring in a continuous feed fixed bed combustor. Commercial software package, ANSYS FLUENT (version 14.5), and MATLAB (version 2012b) are used for the numerical analyses.

Experiments are conducted on a laboratory scale fixed bed combustor. The biomass fuel used in this study is in the form of cylindrical wood pellets. The combustor includes a continuous feeding system. To facilitate temperature measurements fifteen thermocouples are placed axially along the combustor side wall and used to determine the temperature profiles. The thermocouples can be positioned at any desired radial position. A specially designed deflector is positioned at two different

locations in freeboard for the test conditions reported in this study. A continuous sampling gas analyser is used to monitor emissions (O_2, CO, CO_2, NO) and NO_x in the flue gas. A LabView interface (Ver. 2014) has been used to generate a time series of temperatures and emissions data.

In this study, ANSYS Fluent (version 14.5) has been employed to study heat transfer and fluid flow characteristics inside a packed bed and freeboard by implementation of a three-dimensional model of a porous media. Two CFD models have been developed. First model is used for validation against the experimental data and second model is then employed to study the effects of a freeboard deflector. The analyses have been carried out up to 400^{o}C, which covers the temperature range for both particle drying and partially volatile release in biomass combustion.

To facilitate data analysis a MATLAB (Ver. R2012b) script has been developed to post-process the combustion variables including thermocouple, gas analyser and weighting system data. This MATLAB program has been used to derive the percentile mean deviation for each parameter and extract the steady state time period for each test. Another MATLAB script has been developed to investigate the radiative effects on thermocouples. This program compare two numerical model (aspirated and bare bead) to establish the radiation corrected temperature for any thermocouple. More details about the methodologies for the experimental and numerical studies are presented in Chapter 2 and Appendix D.

1.13 Thesis structure

This thesis is presented and organised as "Thesis with publication" format[1]; and is structured in chapters as follows:

Chapter 1 presents the general overview of the project topic and practical applications of biomass combustion and deflectors, followed by project motivations, objectives of the thesis and methodology used in this research.

[1] "Thesis with Publication" is an acceptable format of thesis for postgraduate research at ECU policy. The current thesis has been written based on the guideline provided at http://www.ecu.edu.au/GPPS/policies_db/policies_view.php?rec_id=0000000434. In this format, the submitted thesis can consist of publications that have already been published, are in the process of being published, or a combination of these.

Chapter 2 provides a detailed methodology for processing experimental fixed bed combustor data and defining the steady state time period and effects of a freeboard deflector on the stabilization of the combustion process. The significance of the radiation heat losses (from the surfaces of thermocouple) and its effect on the accuracy of measured temperatures are discussed. Furthermore, the thermal effect of deflectors on the method used to process thermocouple data discussed.

Chapter 3 discusses the effect of deflectors on thermal conversion (burning rate), centreline and near-wall temperature profiles and gaseous emissions (NO, CO, CO_2).

Chapter 4 discusses the effect of deflectors on the flue gases availability and exergy analyses in the fixed bed combustor.

Chapter 5 discusses results from numerical simulation to better understand the effect of freeboard deflectors on pressure drop and heat transfer inside non-reacting packed bed columns.

Chapter 6 provides a general discussion of the results presented in each chapter and addresses the research questions for the overall project.

Chapter 7 integrates the findings of all chapters and also outlines directions for future research.

1.14 Chapter references

1. Calderon, C., *Europian bioenergy outlook, statistical report,* 2012, The European Biomass Association (AEBION): Brussels. p. 28.
2. Quaak, P., Knoef, H., and Stassen, H., *Energy from biomass, A review for combustion and gasification technologies*. Vol. 23. 1999, Washington, D.C.: World Bank Publications. p. 2-5.
3. Bauen, A., Berndes, G., Junginger, M., Londo, M., Vuille, F., Ball, R., Bole, T., Chudziak, C., Faaij, A., and Mozaffarian, H., *Bioenergy – A sustainable and reliable energy source areview of status and prospects.* Report jointly prepared for IEA Bioenergy by the Energy Research Centre of the Netherlands (ECN), E4tech, Chalmers University of Technology, and the Copernicus Institute of the University of Utrecht., 2009.
4. Bauen, A., Howes, J., Bertuccioli, L., Chudziak, C., *Review of the potential for biofuels in aviation.* Final report for Committee on Climate Change, E4tech, 2009.
5. Palmer, D., Tubby, I., Hogan, G., and Rolls, W., *Biomass heating: a guide to medium scale wood chip and wood pellet systems.* Biomass Energy Centre, Farnham, Surrey, 2011.
6. Van Loo, S., and Koppejan, J., *International energy agency bioenergy agreement- Task 19, Biomass combustion,* in *Biomass Combustion Modelling Workshop*2000: Sevilla, Spain.
7. Bridgwater, A.V., *Renewable fuels and chemicals by thermal processing of biomass.* Chemical Engineering Journal, 2003. 91: p. 87-102.
8. Jenkins, B.M., Baxter, L.R., Miles Jr, T.R, and Miles, T.R., *Combustion properties of biomass.* Fuel Processing Technology, 1998. 54: p. 17-46.
9. McKendry, P., *Energy production from biomass (part 1): overview of biomass.* Bioresource Technology, 2002. 83(1): p. 37-46.
10. Hellwig, M., *Basic of the combustion of wood and straw.* International conference on Biomass, Venice , pp. 793-798 (5 ref.), 1985.
11. Van Loo, S. and Koppejan, J., *The handbook of biomass combustion and co-firing*. 2008: Earthscan, UK. 38-50.
12. Gaur, S., Reed, T. B., *An athlas of thermal data for biomass and other fuels* National Renewable Energy Laboratory, U. S. Department of Energy, NREL/TP-433-7965, UC Category:1310, 1995.
13. Prins, M.J., *Thermodynamic analysis of biomass gasification and torrefaction* PhD Thesis, Eindhoven University of Technology, 2005.
14. Rosillo-Calle, F., Groot, P., Hemstock, S. L., and Woods, J., *The biomass assessment handbook, bioenergy for a sustainable environment.* Earthscan, UK, 2007: p. 1-25.
15. ASTM Standard, *E1690-08 Standard test method for determination of ethanol extractives in biomass.* ASTM International, West Conshohocken, PA, 2005. DOI: 10.1520/E1690-08.
16. ASTM Standard, *E1756-08 Standard test method for determination of total solids in biomass.* ASTM International, West Conshohocken, PA, 2005. DOI: 10.1520/E1756-08.
17. ASTM Standard, *E1721-01 Standard test method for determination of acid-insoluble residue in biomass.* ASTM International, West Conshohocken, PA, 2009. DOI: 10.1520/E1721-01.

18. ASTM Standard *E1758-01 Standard test method for determination of carbohydrates in biomass by high performance liquid chromatography*. ASTM International, West Conshohocken, PA, 2007. DOI: 10.1520/E1758-01.
19. ASTM Standard, *E1755-01 Standard test method for ash in biomass.* ASTM International, West Conshohocken, PA, 2007. DOI: 10.1520/E1755-01.
20. ASTM Standard, *E1757-01 Standard practice for preparation of biomass for compositional analysis.* ASTM International, West Conshohocken, PA, 2007. DOI: 10.1520/E1757-01.
21. ASTM Standard, *E873-82 Standard test method for bulk density of densified particulate biomass fuels.* ASTM International, West Conshohocken, PA, 2006. DOI: 10.1520/E0873-82R06.
22. ASTM Standard, *E870-82 Standard test methods for analysis of wood fuels.* ASTM International, West Conshohocken, PA 2006. DOI: DOI: 10.1520/E0870-82R06.
23. ASTM Standard, *E1534-93 Standard test method for determination of ash content of particulate wood fuels.* ASTM International, West Conshohocken, PA, 2006. DOI: 10.1520/E1534-93R06
24. *Australian/New Zealand Standard, AS/NZS 4014.6:2007, Domestic solid fuel burning appliances-test fuels, part 6: wood pellets, ISBN 0 7337 8049 0* 2007.
25. Linda, T., *Ash particle formation mechanisms during pulverised and fluidised bed combustion of solid fuels.* PhD Thesis, Helsinki University of Technology (Espoo, Finland), 1999.
26. *How can biomass be used for energy?, Task 29: IEA Bioenergy Network on Socio-economics; International Energy Agency*. [cited 2013 05/Feb]; Available from: http://www.aboutbioenergy.info/technologies_combustion.html.
27. Shynya, Y. and Yukihiko, M., *The Asian biomass handbook, A guide for biomass production and utilization*. 2006, Tokyo, Japan: The Japan Institute of Energy. p. 207-222.
28. Bovy, P., *Effect of air preheating in moving grate furnaces: modeling convective drying and experimental investigation of spontaneous ignition.* MSc thesis, Eindhoven University of Technology, Department of Mechanical Engineering, Group of Combustion Technology, 2008, Master.
29. Alakangas, E., Flyktman, M., *Biomass CHP technologies.* VTT Energy Report, Finland, 2001.
30. Thunman, H., and Leckner, B., *Co-current and counter-current fixed bed combustion of biofuel-a comparison.* Fuel, 2003. 82: p. 275- 283.
31. Yang, Y.B., Ryu, C., Khor, A., Yatesb, N.E., Sharifi, V.N., and Swithenbank, J., *Effect of fuel properties on biomass combustion. Part II. Modelling approach-identification of the controlling factors.* Fuel, 2005. 84(16): p. 2116-2130.
32. Wurzenberger, J.C., Wallner, S., and Raupenstrauch, H., *Thermal conversion of biomass: comprehensive reactor and particle modeling.* AIChE Journal, 2002. 48(10): p. 2398-2411.
33. Porteiro, J., Patiño, D., Moran, J., and Granada, E., *Study of a fixed-bed biomass combustor: Influential parameters on ignition front propagation using parametric analysis.* Energy and Fuels, 2010. 24(7): p. 3890-3897. DOI: 10.1021/ef100422y.

34. Shin, D. and Choi, S., *The combustion of simulated waste particles in a fixed bed.* Combustion and Flame, 2003. 121: p. 167-180.
35. Katunzi, M., *Biomass conversion in fixed bed experiments, Report number WVT 2006.18,* 2006, Eindhoven University of Technology, Department of Mechanical Engineering: Netherlands. p. 1-55.
36. Saastamoinena, J.J., Taipalea, R., Horttanainenb, M., and Sarkomaab, P., *Propagation of the ignition front in beds of wood particles.* Combustion and Flame, 2000. 123(1-2): p. 214-226.
37. Van Kessel, L.B.M., Arendsen, A.R.J., de Boer-Meulman, P.D.M., and Brem, G., *The effect of air preheating on the combustion of solid fuels on a grate.* Fuel 2004. 83(9): p. 1123-1131.
38. Gort, R., and Brouwers, J. J., *Theoretical analysis of the propagation of a reaction front in a packed-bed.* Combustion and flame, 2001. 124: p. 1-13.
39. Gort, R., *On the propagation of a reaction front in a packed bed: thermal conversion of municipal waste and biomass* PhD Thesis, Universiteit Twente, Enschede, 1995.
40. Yang, Y.B., Yamauchi, H., Sharifi, V.N., and Swithenbank, J., *Effect of moisture on the combustion of biomass and simulated solis waste in a packed bed.* Journal of the Energy Institute, 2003. 76: p. 105-15.
41. Saastamoinen, J.J., Horttanainen, M., and Sarkomaa, P., *Ignition wave propagation and release of volatiles in beds of wood particles.* Combustion Science and Technolgy, 2001. 165(1): p. 41-60.
42. Doherty, W., Reynolds,A, and Kennedy, D., *The effect of air preheating in a biomass CFB gasifier using ASPEN Plus simulation.* Biomass and Bioenergy, 2009. 33: p. 1158-1167.
43. Dong, W., and Blasiak, W., *Study on mathematical modeling of highly preheated air combustion.* The 2nd High Temperature Air Combustion Symposium, Taiwan, 1999.
44. Salzmann, R., *Fuel Staging for NOx Reduction in Biomass Combustion: Experiments and Modeling.* Energy & Fuels, 2001. 15: p. 575-582.
45. Wiinikka, H., and Gebart, R., *The influence of air distribution rate on particle emissions in fixed bed combustion of biomass.* Combustion Science and Technology, 2005. 177(9): p. 1747-1766. DOI: 10.1080/00102200590959468.
46. Klason, T., Bai, X.S., Bahador, M., Nilsson, T.K., and Sunden, B., *Investigation of radiative heat transfer in fixed-bed biomass furnaces.* Fuel, 2008. 87(10): p. 2141-2153.
47. Siegel, R., and Howell, J. R., *Thermal radiation heat transfer.* Taylor & Francis, 4th edition, US, 2002: p. 419-490.
48. Nilsson, T., and Sunden, B., *Numerical analysis of radiation heat transfer in combustion of bio fuels.* Advanced Computational Methods in Heat Transfer, WIT Press, ISBN 1-85312-818-X, 2000.
49. Klippel, N., and Nussbaumer, T., *Health relevance of particles from wood combustion in comparison to diesel soot.* 15th European Biomass Conference, Berlin, 2007.
50. Kovacevik, B., *Alkali-containing aerosol particles release during biomass combustion and ambient air concentrations.* PhD Thesis, University of Gothenburg, Department of Chemistry, Atmospheric Science, 2009.
51. Abbott, J., Stewart, R., Fleming, S., Stevenson, K., Green, J., and Coleman, P., *Measurement and modelling of fine particulate emissions (PM10 &*

PM2.5) from wood-burning biomass boilers. Report to The Scottish Government, AEA Energy & Environment Glengarnock Technology Centre, 2008.
52. Obernberger, I., Brunner, T., and Barnthaler, G., *Fine particle emissions from modern Austrian small scale biomass combustion plants.* 15th European Biomass Conference and Exhibition, Germany, 2007.
53. Glanville, P., E. and Kirby, M., J, *Use of computational fluid dynamics to reduce particulate emissions from wood-fired hydronic furnace.* Technical Report, University of Washington, Department of Mechanical Engineering, 2008.
54. Porle, K., Klippel, N., Riccius, O., Kauppinen, I. I., and Lind, T., *Full scale ESP performance after PC-boilers firing low sulfur coals.* Proceedings of EPRI/DOE International Conference of Managing Hazardous and Particulate Air Pollutants, Toronto, Canada, 1997.
55. Salaver, L., Lee, T., Cooper, C.D., Yu Wu, C., and Donnelly, J., *Air pollution emission control devices for stationary sources.* Air & Waste Management Association (A&WMA), 2007.
56. Buczynski, R., *Investigation of fixed-bed combustion process in small scale boilers.* Faculty of Environmental Engineering and Energy, Silesian University of Technology and Clausthal University of Technology, Gliwice, Poland, 2011, Doctoral thesis.
57. Charles, E.B., *Heat transfer in industrial combustion.* CRC Press LLC, US, 2000: p. 345-367.
58. Wiinikka, H., and Gebart, R., *Critical parameters for particle emissions in small-scale fixed-bed combustion of wood pellets.* American Chemical Society Journal, 2004. 18: p. 898-907.
59. Katunzi, M., *Biomass conversion: Literature review and fixed bed experiments.* System integration project 2, Eindhoven University of Technology, 2005.
60. Rogaumea, T., Auzanneau, M., Jabouille, F., Goudeau, J.C., and Torerob, J.L., *The effects of different airflows on the formation of pollutants during waste incineration.* Fuel, 2002. 81: p. 2277-2288.
61. Yin, C., Rosendahl, L., Kaer, S. K., Clausen, S., Hvid, S. L., and Hille, T., *Mathematical Modeling and Experimental Study of Biomass Combustion in a Thermal 108 MW Grate-Fired Boiler.* Energy and Fuels, 2008. 22: p. 1380-1390.
62. Van Kuijk, H.A.J.A., *Grate furnace combustion: A model for the solid fuel layer.* PhD Thesis, Eindhoven University of Technology, 2008: p. 69-78.
63. Wurzenberger, C., Wallner, S., and Raupenstrauch, H., *Thermal conversion of biomass: comprehensive reactor and particle modeling.* AIChE Journal, 2002. 48(10): p. 2398–2411.
64. Nicholls, P., *Underfeed combustion, effect of preheat, and distribution of ash in fuel beds.* Bulletin of the United States Bureau of Mines, 1934. 378.
65. Van der Lans , R.P., Pedersen, L.T., Jensen, A., Glarborg, P., and Johansen, D., *Modelling and experiments of straw combustion in a grate furnace.* Biomass and Bioenergy, 2000. 19: p. 199-208.
66. Samuelsson, J.I., *Conversion of nitrogen in a fixed buring biofuel bed.* Thesis for the degree of licentiate of engineering, Chalmers University of Technology, 2006.

67. Weissinger, A., Fleckl, T., Obernberger, I., *In situ FT-IR spectroscopic investigations of species from biomass fuels in a laboratory-scale combustor: the release of nitrogenous species.* Combustion and Flame, 2004. 137(4): p. 403-417.
68. Yang , Y.B., Sharifi, V.N., and Swithenbank, J., *Effect of air flowrate and fuel moisture on the burning behaviors of biomass and simulated municipal solid wastes in packed beds.* Fuel, 2004. 83(11): p. 1553-1562.
69. Ryu, C., Yang, Y. B., Khor, A., Yates, N., Sharifi, V.N., and Swithenbank, J., *Effect of fuel properties on biomass combustion: Part 1. Experiments-fuel type, equivalence ratio and particle size.* Fuel, 2006. 85: p. 1039-1046.
70. Ryu, C., Phan, A.N., Sharifi, V.N., and Swithenbank, J., *Combustion of textile residues in a packed bed.* Experimental Thermal and Fluid Science, 2007. 31(8): p. 887-895.
71. Zhou, H., *Numerical modelling of straw combuster in a fixed Bed.* Fuel, 2004. 84: p. 389-403.
72. Porteiro, J., Granada, E., Collazo, J., Patiño, D., and Morán, J., *Exprimental analysis of ingnition front of several biomass fuel in a fixed-bed combuster.* Fuel, 2010. 89(1): p. 26-35.
73. Ryan, J.S. and Hallett, W.L., *Packed bed combustion of char particles: experiments and an ash model.* Chemical Engineering Sience, 2002. 57: p. 3873-3882.
74. Zhao, W., Li, Z., Wang, D., Zhu, K., Sun, R., Meng, B., and Zhao, G., *Combustion characteristics of different parts of corn straw and NO formation in a fixed bed.* Bioresource Technology, 2008. 99(8): p. 2956-2963.
75. Rönnbäck, M., Axell, M., Gustavsson, L., Thunman, H., and Lecher, B., *Combustion Processes in a Biomass Fuel Bed-Experimental Results.* Proceeding of Progress in thermochemical biomass conversion, Tyrol, Austria, 2000: p. 743-757.
76. Horttanainen, M., Saastamoinen, J., and Sarkomaa, P., *Operational limits of ignition front propagation against airflow in packed beds of different wood fuels.* Energy and Fuels, 2002. 16: p. 676-686.
77. Fatehi, M. and Kaviany, M., *Adiabatic Reverse Combustion in a Packed bed.* Combustion and flame, 1994. 99: p. 1-17.
78. Pérez, J.F., Benjumea, P.N., and Melgar, A., *Sensitivity analysis of a biomass gasification model in fixed bed downdraft reactors: Effect of model and process parameters on reaction front.* Biomass and Bioenergy, 2015. 83: p. 403-421.
79. Febrero, L., Granada, E., Patiño, D., Eguía, P., and Regueiro, A., *A Comparative Study of Fouling and Bottom Ash from Woody Biomass Combustion in a Fixed-Bed Small-Scale Boiler and Evaluation of the Analytical Techniques Used.* Sustainability, 2015. 7(5): p. 5819-5837.
80. Wiinikka, H., *High temperature aerosol formation and emission minimisation during combustion of wood pellets.* PhD Thesis, Luleå University of Technology, 2005: p. 37-75.
81. Wiinikka, H., Gebart, R., Boström, C., and Dan Öhman, M., *Influence of fuel ash composition on high temperature aerosol formation in fixed bed combustion of woody biomass pellets.* Fuel, 2007. 86(1-2): p. 181-193. DOI: 10.1016/j.fuel.2006.07.001.

82. Houshfar, E., Khalil, R.A., Løvås, T., and Skreiberg, Ø., *Enhanced NO x reduction by combined staged air and flue gas recirculation in biomass grate combustion.* Energy & Fuels, 2012. 26(5): p. 3003-3011.
83. Pettersson, E.r., Lindmark, F., Öhman, M., Nordin, A., Westerholm, R., and Boman, C., *Design changes in a fixed-Bed pellet combustion device: effects of temperature and residence time on emission performance.* Energy & Fuels, 2010. 24(2): p. 1333-1340.
84. Munir, S., Nimmo, W., and Gibbs, B., *The effect of air staged, co-combustion of pulverised coal and biomass blends on NOx emissions and combustion efficiency.* FUEL, 2011. 90(1): p. 126-135.
85. Sami, M., Annamalai, K., Dhanapalan, S. and Wooldridge, M., *Numerical simulation of blend combustion of coal and feedlot waste in a swirl burner.* ASME conference, Nashville, TN, 1999.
86. Scharler, R., Obernberger, I., Längle, G. and Heinzle, J., *CFD analysis of air staging and flue gas recirculation in biomass grate furnace.* Proceeding of the 1st World Conference on Biomass for Energy and Industry, Sevilla, Spain, 2000.
87. Scharler, R., Forstner, R., M., Braun, M., Brunner, T, and Obernberger. I, *Advanced CFD analysis of large fixed bed biomass boilers with special focus on the convective section.* 2nd World Conference and Exhibition on Biomass for Energy, Industry and Climate Protection, Rome, Italy, 2004.
88. Yang, Y.B., Yamauchi, H., Sharifi. V. N., and Swithenbank, J., *Effects of fuel devolatilisation on the combustion of wood chips and incineration of simulated municipal solid wastes in a packed bed.* Fuel, 2003. 82(18): p. 2205-2221.
89. Yang, Y.B., Ryu, C., Khor, A., Sharifi, V. N., and Swithenbank, J., *Fuel size effect on pinewood combustion in a packed bed.* Fuel, 2005. 84: p. 2026–2038.
90. Yang, Y.B., Goodfellow, J., Sharifi, V. N., and Swithenbank, J., *Investigation of biomass combustion systems using CFD techniques: a parametric study of packed-bed burning characteristics.* Progress in Computational Fluid Dynamics, 2006: p. 262-271.
91. Yang, Y.B., Newman, R., Sharifi, V. N., Swithenbank, J., Ariss, J., *Mathematical modelling of straw combustion in a 38 MWe power plant furnace and effect of operating conditions.* Fuel, 2007. 86: p. 129-142.
92. Ryu, C., Phan, A. N., Yang, Y, Sharifi, V. N. and Swithenbank, J., *Swithenbank. Ignition and burning rates of segregated waste combustion in packed beds.* Waste management, 2007: p. 802-810.
93. Yin, C., Rosendahl, L., and Condra, T. J., *Further study of the gas temperature deviation in large-scale tangentially coal-fired boiler.* Fuel, 2003. 82: p. 1127-1137.
94. Yin, C., Rosendahl, L., Kaer, S. K., and Condra, T. J., *Use of numerical modeling in design for co-firing biomass in wall-fired burners.* Chemical Engineering Science, 2004. 59: p. 3281-3292.
95. Yin, C., Rosendahl, L, and K. Kaer, S, *Grate-firing of biomass for heat and power production.* Progress in Energy and Combustion Science, 2008. 34: p. 725-754.
96. Rosendahl, L.A., Yin, C., Kaer, S. K., Friborg, K., and Overgaard, P., *Physical characterization of biomass fuels prepared for suspension firing*

in utility boilers for CFD modeling. Biomass and Bioenergy, 2007. 31: p. 318-325.
97. Kaer, S.K., *Numerical modeling of a straw-fired grate boiler.* Fuel, 2004. 83: p. 1183-1190.
98. Kaer, S.K., Rosendahl, L. A., and Baxter, L. L., *Towards a CFD-based mechanistic deposit formation model for straw-fired boilers.* Fuel, 2006. 85: p. 833-848.
99. Wei, D., and Blasiak, W. , *CFD modeling of ecotube system in coal and waste grate combustion.* Energy Conversion and Management, 2001. 42(15-17): p. 1887-1896.
100. Yu, Z., Ma, X., and Liao, Y., *Mathematical modeling of combustion in a grate-fired boiler burning straw and effect of operating conditions under air- and oxygen-enriched atmospheres.* Renewable Energy, 2010. 35(5): p. 895-903.
101. Ryu, C., Phan, A., Yang, Y.B., Sharifi, V.N., and Swithenbank, J., *Ignition and burning rates of segregated waste combustion in packed beds.* Waste Management, 2006. 27(6): p. 802-810.
102. Nussbaumer, T., Czasch, C., Klippel, N., Johansson, J., and Tullin, C. *Primary and secondary measures for the reduction of nitric oxide emissions from biomass combustion.* in Developments in Thermochemical Biomass Conversion. 1996. Springer Netherlands. p. 1447-1461.
103. Porteiro, J., Granada, E., Collazo, J., Patino, D., and Moran, J., *Study of the reaction front thickness in a counter-current fixed-bed combustor of a pelletised biomass.* Combustion and Flame, 2012. 159(3): p. 1296-1302.
104. Yang., Y.B., Sharifi, V. N., and Swithenbank, J., *Substoichiometric conversion of biomass and solid wastes to energy in packed beds.* AIChE Journal, 2006. 52(2): p. 809-817. DOI: 10.1002/aic.10646.
105. Ganapathy, V., *Industrial boilers and heat recovery steam generators: design, applications, and calculations*. 2002, Texas, USA: CRC Press. p. 139-165.
106. Buczyński, R., Weber, R., and Szlęk, A., *Innovative design solutions for small-scale domestic boilers: Combustion improvements using a CFD-based mathematical model.* Journal of the Energy Institute, 2015. 88(1): p. 53-63.
107. Ryfa, A., Buczynski, R., Chabinski, M., Szlek, A., and Bialecki, R.A., *Decoupled numerical simulation of a solid fuel fired retort boiler.* Applied Thermal Engineering, 2014. 73(1): p. 794-804.
108. Khodaei, H., Al-Abdeli, Y.M., Guzzomi, F., and Yeoh, G.H., *An overview of processes and considerations in the modelling of fixed-bed biomass combustion.* Energy, 2015. 88: p. 946-972.
109. Logtenberg, S.A. and Dixon, A., *Computational fluid dynamics studies of fixed bed heat transfer.* Chemical Engineering and Processing: Process Intensification, 1998. 37(1): p. 7-21.
110. Achenbach, E., *Heat and flow characteristics of packed beds.* Experimental Thermal and Fluid Science, 1995. 10(1): p. 17-27.
111. Bey, O. and Eigenberger, G., *Gas flow and heat transfer through catalyst filled tubes.* International Journal of Thermal Sciences, 2001. 40(2): p. 152-164.

112. du Toit, C.G., and Rousseau, P.G., *Modeling the flow and heat transfer in a packed bed high temperature gas-cooled reactor in the context of a systems CFD approach.* Journal of Heat Transfer, 2012. 134(3): p. 1-12.
113. Hawthorn, R., Ackerman, G., and Nixon, A., *A mathematical model of a packed-bed heat-exchanger reactor for Dehydrogenation of Methylcyclohexane: Comparison of predictions with experimental results.* AIChE Journal, 1968. 14(1): p. 69-76.
114. Porteiro, J., Granada, E., Collazo, J., Patino, D., Moran, and Miguez, J., *Numerical modeling of a biomass pellet domestic boiler.* Energy and Fuels, 2009. 23: p. 1067-1075.
115. Collazo, J., Porteiro, J., Miguez, J. L., Granada, E., and Gomez, M. A., *Numerical simulation of a small scale biomass boiler.* Energy Conversion and Management, 2012. 64: p. 87-96.
116. Patiño, D., Moran, J., Porteiro, J., Collazo, J., Granada, E, and Miguez, J., *Improving the cofiring process of wood pellet and refuse derived fuel in a small-scale boiler plant.* Energy and Fuels, 2008. 22(3): p. 2121-2128.
117. Li, P.W., Van Lew, J., Karaki, W., Chan, C.L., Stephens, J., and O'Brien, J.E., *Transient Heat Transfer and Energy Transport in Packed Bed Thermal Storage Systems.* Developments in Heat Transfer, InTech, 2011: p. 374-416.
118. Hughes, P.J., Klein, S.A., and Close, D.J., *Packed bed thermal storage models for solar air heating and cooling systems.* Journal of Heat Transfer, 1976. 98(2): p. 336-338.
119. Villatoro, F., Pérez, J., Domínguez-Muñoz, F., and Cejudo-López, J., *Approximate analytical solution for the heat transfer in packed beds for solar thermal storage in building simulators.* In Eleventh International IBPSA Conference, Glasgow, Scotland, July 2009: p. 709-715.
120. Critoph, R., *Forced convection adsorption cycle with packed bed heat regeneration: Cycle à adsorption à convection forcée avec régénération thermique du lit fixe.* International Journal of Refrigeration, 1999. 22(1): p. 38-46.
121. Renken, K.J. and Poulikakos, D., *Experiment and analysis of forced convective heat transport in a packed bed of spheres.* International Journal of Heat and Mass Transfer, 1988. 31(7): p. 1399-1408.
122. Peters, B., Schröder, E., Bruch, C., and Nussbaumer, T., *Measurements and particle resolved modelling of heat-up and drying of a packed bed.* Biomass and Bioenergy, 2002. 23(4): p. 291-306.
123. Logtenberg, S., Nijemeisland, M., and Dixon, A., *Computational fluid dynamics simulations of fluid flow and heat transfer at the wall–particle contact points in a fixed-bed reactor.* Chemical Engineering Science, 1999. 54(13): p. 2433-2439.
124. Nijemeisland, M. and Dixon, A., *CFD study of fluid flow and wall heat transfer in a fixed bed of spheres.* AIChE Journal, 2004. 50(5): p. 906-921.
125. Guardo, A., Coussirat, M., Larrayoz, Larrayoz, A.M., Recasens, F., and Egusquiza, E., *CFD flow and heat transfer in nonregular packings for fixed bed equipment design.* Industrial & Engineering Chemistry Research, 2004. 43(22): p. 7049-7056.
126. Romkes, S., Dautzenberg, F.M., Van den Bleek, C.M., and Calis, H., *CFD modelling and experimental validation of particle-to-fluid mass and heat transfer in a packed bed at very low channel to particle diameter ratio.* Chemical Engineering Journal, 2003. 96(1): p. 3-13.

127. Zili, L. and Nasrallah, S.B., *Heat and mass transfer during drying in cylindrical packed beds.* Numerical Heat Transfer: Part A: Applications, 1999. 36(2): p. 201-228.
128. Pianko-Oprych, P., *Modelling of heat transfer in a packed bed column.* Polish Journal of Chemical Technology, 2011. 13(4): p. 34-41.
129. Beveridge, G. and Haughey, D., *Axial heat transfer in packed beds. Gas flow through beds between 20 and 650 C.* International Journal of Heat and Mass Transfer, 1972. 15(5): p. 953-968.
130. Beveridge, G.S.G. and Haughey, D.P., *Axial heat transfer in packed beds. Stagnant beds between 20 and 750 C.* International Journal of Heat and Mass Transfer, 1971. 14(8): p. 1093-1113.
131. Votruba, J., Hlaváček, V., and Marek, M., *Packed bed axial thermal conductivity.* Chemical Engineering Science, 1972. 27(10): p. 1845-1851.
132. Guardo, A., Coussirat, M., Recasens, F., Larrayoz, M.A. and Escaler, X, *CFD study on particle-to-fluid heat transfer in fixed bed reactors: Convective heat transfer at low and high pressure.* Chemical Engineering Science, 2006. 61(13): p. 4341-4353.
133. Varunkumar, S., Rajan, N., and Mukunda, H., *Universal flame propagation behavior in packed bed of biomass.* Combustion Science and Technology, 2013. 185(8): p. 1241-1260.
134. Salzmann, R. and Nussbaumer, T., *Fuel staging for NO x reduction in biomass combustion: experiments and modeling.* Energy & Fuels, 2001. 15(3): p. 575-582.
135. Klason, T. and Bai, X., *Computational study of the combustion process and NO formation in a small-scale wood pellet furnace.* Fuel, 2007. 86(10): p. 1465-1474.
136. Brohez, S., Delvosalle, C., and Marlair, G., *A two-thermocouples probe for radiation corrections of measured temperatures in compartment fires.* Fire Safety Journal, 2004. 39(5): p. 399-411.
137. Roberts, I.L., Coney, J.E.R., and Gibbs, B.M., *Estimation of radiation losses from sheathed thermocouples.* Applied Thermal Engineering, 2011. 31(14): p. 2262-2270.
138. Luo, M. and Beck, V., *The fire environment in a multi-room building—comparison of predicted and experimental results.* Fire Safety Journal, 1994. 23(4): p. 413-438.
139. Pitts, W.M., Braun, E., Peacock, R.D., Mitler, H.E., Johnson, E., Reneke, P.A., and Blevins, L.G., *Temperature uncertainties for bare-bead and aspirated thermocouple measurements in fire environments.* ASTM Special Technical Publication, 2003. 1427: p. 3-15.
140. Heitor, M. and Moreira, A., *Probe measurements of scalar properties in reacting flows.* Combustings Flow Diagnostics, 1992: p. 79-136.

At the author's request,

Chapters 2, 3, 4, and 5

have not been included in this version of the thesis.

Chapter 6

General discussion

Although deflectors have been used in the freeboard section of the industrial furnaces to reduce particle matters and flame radiation into the exhaust stack, their impact on emissions and temperature distributions, remains one of the outstanding challenges in the biomass combustors. Whilst no systematic studies into the effects of freeboard deflectors has been made, published work indicates that wall temperatures and flow dynamics in the freeboard section affect the emissions, particulate matters and residence time [1-3].

The main aim of this chapter is to integrate the research outcomes to help build a better overall picture in this area. In this way, this chapter will not only establish connections among the chapters, but will also address the research questions presented in Chapter 1.

6.1 Defining the one set of steady state

Although most published research reported results are based on the steady state operating behaviour, there are challenges associated with defining this stage. The temporal stabilization of the thermocouple and emissions data was investigated for the tests with and without deflector in Chapter 2 and a new method for extracting the steady state time period has been proposed. The results showed by driving the percentile mean deviation (Figures 2.6 and 2.8) for the temperature and species data, and selecting various time spans, the steady state operating period can be more accurately specified in comparison to simply using the raw time series data of temperatures and emissions (Figure 2.3). The presence of a freeboard deflector appears to delay stabilization of the percentile deviation of temperatures, particularly in the downstream. It also appears the burning rate is not a sensitive indicator to establish the steady state time window (Figure 2.2).

6.2 Radiative heat transfer from the thermocouple surface

The measured gas temperature can be affected by radiation heat loss from the surface of the thermocouple to the surrounding reactor walls and which subsequently affects the accuracy of measured temperature. Numerical simulations [4] and experimental results [5, 6] have revealed that thermocouples are more likely to be affected by radiation (loss) to the walls than radiative (gain) with the fuel bed. Bare bead thermocouples show the maximum temperature measurement error compared to the sheathed and single shielded aspirated thermocouples [7, 8], therefore these two extreme corrections (bare bead and single shielded aspirated models) have been chosen to estimate radiation compensations for the experimental configuration used (Figure 2.10). It appears that radiative effects have greater impact on the thermocouples in the vicinity of the secondary air zone (Figure 2.11). This may be due to the cooling effect resulting from the secondary air flows. It also appears the presence of the deflector reduces the radiation errors for the thermocouples which located in the downstream. Because of the deflector effects on the wall temperatures and radial temperature profiles in the downstream. Results conclude the significance of the radiation heat losses are negligible for the tests conducted on this laboratory scale combustor.

6.3 Effects of deflectors on combustion performance

6.3.1 Emissions

The data have been banded into three ranges of stoichiometry ($\lambda_{primary}$=0.317-0.423, 0.439-0.509, and 0.537-0.607). The range of $\lambda_{primary}$=0.439-0.509 is focussed upon because of an agglomeration of data points (Table 3.2 and Figure 3.3). These data cover tests with deflector at two axial distances (H=240 and 425mm) as well as baseline tests with no deflector. Results showed using a deflector generally increase the level of CO emissions (Figure3.6b) but leads to a decrease in the average NO and CO_2 emissions (Figures 3.6a and 3.3). It should be noted that the deflector effects are also sensitive to its location as shown by data at H=240mm and 245mm. Parameters such as fuel quality [9], excess air (staging) [2, 9-12], fuel staging [13], temperature and fluid dynamics [14] affect NO and CO formation. Since the experimental results confirm the reduction in the average downstream temperatures (Figures 3.5a and 3.5b) and temperature ranges are too low for thermal NO

formation (T>1300^{o}C), therefore fuel-N conversion is the dominant mechanism for NO generation [1, 2, 12, 15]. Bear in mind that the deflectors affect the fluid flow upstream of the deflectors through longer residence time, it seems the effect of the deflector on NO and CO emissions is due to flue gas mixing and turbulence behaviour in the downstream section.

6.3.2 Temperatures

The presence of a deflector at H=240mm (upstream of the secondary air) decreases the near-wall temperature profiles upstream of the secondary air (TC13 to TC7, Figure 3.5a) on the contrary, the temperatures increase in the downstream of the secondary air (TC6 to TC0). Positioning the deflector at H=425mm (downstream of the secondary air) decrease its influence on the downstream near-wall temperatures (TC6-TC0). Results showed the magnitude of change in upstream wall temperatures (TC13-TC7) is sensitive to deflector distance (H). It can be concluded that the presence of a deflector whether upstream or downstream of the secondary air reduces downstream near-wall temperatures (TC6-TC0). The reasons for this behaviour could be due to the varied flow conditions and residence time (in the upstream) [16]. The deflector appears to affects the centreline temperature profiles in the upstream (TC13-TC7) but no clear effects have been seen in the downstream (TC6-TC0) as presented in the Figure 3.5c.

6.3.3 Burning rate

Despite the deflector effects on emissions and temperatures, they don't have a significant impact on the burning rate. Figure 3.4a shows very similar fuel consumption rate (kgs^{-1}) over time for a range of test cases, both with and without a deflector over $\lambda_{primary}$=0.439-0.509. The burning rate is established across all the data which which are acquired (at 600sec intervals) over a lengthy period of testing. Its steadiness also means it is invalid to use as an indicator for the start of the steady state performance.

6.3.4 Flue gases availability

Results show that deflectors do not have significant impacts on the total exergy and CO chemical exergy of the flue gases at the exhaust section (Figure 4.6). However, the mechanical exergy profiles inside the combustor are affected by the use of

freeboard deflectors (Figure 4.5). Presence of a deflector appears to decrease the mechanical exergy profiles downstream of the secondary air. Impacts of deflector on the mechanical exergy are sensitive to deflector location (H). Deflectors located downstream of the secondary air at H=425mm have more impact on upstream mechanical exergy.

6.4 Effects of deflectors on the heat transfer inside non-reactive packed bed columns

6.4.1 Effects of deflectors on the axial temperature profiles

Several equations have been derived for the effective thermal conductivity based on their respective experimental conditions [17-21]. To obtain representative values of the steady-state effective thermal conductivity for each of the eleven zones, preliminary simulations are carried out against the original data [22]. Simulations were carried out for a temperature range of 100-400°C which is typical for drying and volatile release in biomass combustion. Numerical results showed with constant wall temperature boundary condition (wall heated), deflectors have no significant impact on the centreline axial temperature profile inside the bed and freeboard (Figure 5.6). To understand the effects of deflector on temperature distribution inside the packed bed with heated inlet air the simulations with the new boundary condition have been performed. The inlet air temperature was set at 400^{o}C and the wall of packed bed and freeboard are assumed to be uninsulated and heat transfer is due to convection and radiation from the walls other boundary conditions are same as previous models. It is seen that in this case deflector is not only affects axial temperature within the freeboard, but also changes axial temperature profile inside the packed bed (Figure 5.7). Results revealed that the deflector position (H) does not appear to influence the intra-bed temperatures, which is expected. However, for both deflector positions (H=10mm or H=185mm), the freeboard deflector leads to a ~5% increase in temperature within the freeboard. This temperature change inside the freeboard is likely to be attributed to the convective and radiative effect from the deflector (Figure 5.6).

6.4.2 Effects of deflectors on the radial temperature distributions

The results depend on the mode of heating. Simulations were carried out for two boundary conditions: (i) heated walls by assuming constant temperature at the

exterior walls and (ii) heated inlet air. CFD results predicted that in wall-heated packed beds, deflectors have minimal impact on the radial temperature distributions inside the bed (Figures 5.8a and 5.8d). However, they change radial temperature profiles and increase the near-wall temperatures (Figures 5.8b, 5.8c, 5.8e and 5.8f). At stream temperatures of 100°C, the presence of a deflector leads to an increase of ~5% (Figure 5.8c) but this increase to ~7% at 400°C (Figure 5.8f).

For the temperature range investigated (100°C to 400°C), the results reveal that deflectors have significant effects on the temperature distributions in the freeboard by increasing the wall temperature. However, the impacts of deflectors on the temperature profiles inside the packed bed are negligible. By changing the boundary conditions and heating the packed bed by increasing the inlet air temperature (instead of constant wall temperature), deflector effects become more pronounced. In this case deflector affects both the temperature distributions inside packed bed and freeboard.

6.5 Chapter references

1. Nussbaumer., T., *Combustion and Co-combustion of Biomass: Fundamentals, Technologies, and Primary Measures for Emission Reduction.* Energy and Fuels, 2003. 17: p. 1510-1521.
2. Houshfar, E., Skreiberg, Ø., Løvås, T., Todorović, D.a., and Sørum, L., *Effect of excess air ratio and temperature on NOx emission from grate combustion of biomass in the staged air combustion scenario.* Energy & Fuels, 2011. 25(10): p. 4643-4654.
3. Eskilsson, D., Rönnbäck, M., Samuelsson, J., and Tullin, C., *Optimisation of efficiency and emissions in pellet burners.* Biomass and Bioenergy, 2004. 27(6): p. 541-546.
4. Klason, T., Bai, X.S., Bahador, M., Nilsson, T.K., and Sunden, B., *Investigation of radiative heat transfer in fixed-bed biomass furnaces.* Fuel, 2008. 87(10): p. 2141-2153.
5. Wiinikka, H., *High temperature aerosol formation and emission minimisation during combustion of wood pellets.* PhD Thesis, Luleå University of Technology, 2005: p. 37-75.
6. Wiinikka, H., Gebart, R., Boman, C., Boström, D., Nordin, A., and Öhman, M., *High-temperature aerosol formation in wood pellets flames: Spatially resolved measurements.* Combustion and Flame, 2006. 147(4): p. 278-293.
7. Pitts, W.M., Braun, E., Peacock, R.D., Mitler, H.E., Johnson, E., Reneke, P.A., and Blevins, L.G., *Temperature uncertainties for bare-bead and aspirated thermocouple measurements in fire environments.* ASTM Special Technical Publication, 2003. 1427: p. 3-15.
8. Blevins, L.G. and Pitts, W.M., *Modeling of bare and aspirated thermocouples in compartment fires.* Fire Safety Journal, 1999. 33(4): p. 239-259.
9. Staiger, B., Unterberger, S., Berger, R., and Hein, K.R., *Development of an air staging technology to reduce NOx emissions in grate fired boilers.* Energy, 2005. 30(8): p. 1429-1438.
10. Munir, S., Nimmo, W., and Gibbs, B., *The effect of air staged, co-combustion of pulverised coal and biomass blends on NOx emissions and combustion efficiency.* FUEL, 2011. 90(1): p. 126-135.
11. Lamberg, H., Sippula, O., Tissari, J., and Jokiniemi, J., *Effects of air staging and load on fine-particle and gaseous emissions from a small-scale pellet boiler.* Energy & Fuels, 2011. 25(11): p. 4952-4960.
12. Mahmoudi, S., Baeyens, J., and Seville, J.P., *NOx formation and selective non-catalytic reduction (SNCR) in a fluidized bed combustor of biomass.* Biomass and Bioenergy, 2010. 34(9): p. 1393-1409.
13. Salzmann, R. and Nussbaumer, T., *Fuel staging for NO x reduction in biomass combustion: experiments and modeling.* Energy & Fuels, 2001. 15(3): p. 575-582.
14. Pettersson, E.r., Lindmark, F., Öhman, M., Nordin, A., Westerholm, R., and Boman, C., *Design changes in a fixed-Bed pellet combustion device: effects of temperature and residence time on emission performance.* Energy & Fuels, 2010. 24(2): p. 1333-1340.
15. Zhou, H., Jensen, A., Glarborg, P., and Kavaliauskas, A., *Formation and reduction of nitric oxide in fixed-bed combustion of straw.* FUEL, 2006. 85(5): p. 705-716.

16. Houshfar, E., Skreiberg, Ø., Todorović, D., Skreiberg, A., Løvås, T., Jovović, A., and Sørum, L., *NOx emission reduction by staged combustion in grate combustion of biomass fuels and fuel mixtures.* FUEL, 2012. 98: p. 29-40.
17. Demirel, Y., Sharma, R., and Al-Ali, H., *On the effective heat transfer parameters in a packed bed.* International Journal of Heat and Mass Transfer, 2000. 43(2): p. 327-332.
18. Bunnell, D., Irvin, H., Olson, R., and Smith, J., *Effective thermal conductivities in gas-solid systems.* Industrial & Engineering Chemistry, 1949. 41(9): p. 1977-1981.
19. Votruba, J., Hlaváček, V., and Marek, M., *Packed bed axial thermal conductivity.* Chemical Engineering Science, 1972. 27(10): p. 1845-1851.
20. Vortmeyer, D. and Adam, W., *Steady-state measurements and analytical correlations of axial effective thermal conductivities in packed beds at low gas flow rates.* International Journal of Heat and Mass Transfer, 1984. 27(9): p. 1465-1472.
21. Yagi, S., Kunii, D., and Wakao, N., *Studies on axial effective thermal conductivities in packed beds.* AIChE Journal, 1960. 6(4): p. 543-546.
22. Wen, D. and Ding, Y., *Heat transfer of gas flow through a packed bed.* Chemical Engineering Science, 2006. 61(11): p. 3532-3542.

Chapter 7

Conclusion and Future Work Recommendations

This chapter integrates the findings of all chapters and offers suggestions for possible future works.

7.1 Conclusions

This thesis largely focused on the impact of freeboard deflectors in fixed bed biomass combustors and non-combusting packed beds. Fixed bed counter-current thermal conversion is investigated due to its similarity with large industrial moving and fixed grate burners. Both experimental and numerical techniques were utilised to address the research questions stated in Chapter 1.

7.1.1 Onset of steady state in combusting packed beds

A new method for defining the onset of steady state in fixed bed combustors has been developed and effects of radiation losses on thermocouples data investigated. In addition, the sensitivity of these outcomes to the presence of downstream deflector is also presented. From the study the following conclusions can be drawn:

- Using the time series of (raw) operating parameters such as the temperature and emissions data or observing visible flame behavior is not a reliable method to identify steady state conditions during the testing of fixed bed biomass combustors.
- Results reveal that using only the burning rate is not a sensitive indicator to determining the start of the steady state period in the continuous feeding fixed bed combustor.
- The use of the percentile mean deviation of temperatures (at multiple axial stations) and NO/CO emissions data can provide a clearer methodology to defining the start of the steady state period.
- Defining the start of the steady state time period is based on the stabilization time of NO/CO or temperatures (whichever takes longer time to stabilize). In the results presented, emissions appearing to stabilize earlier than temperatures.

This is however dependent on the combustion stoichiometry as it affects both temperatures and emissions.

- The stabilization of the percentile deviation of temperatures (particularly in the downstream) is affected by the use of freeboard deflectors. Deflectors cause higher level of fluctuation (R_i) and delay the stabilization of the percentile deviation of temperatures. This maybe attributable to turbulence and/or radiative heat transfer effects associated with freeboard deflector.
- To characterize the significance of correcting thermocouple data for radiative (wall) losses, two numerical models (aspirated and bare bead) were compared. The results show that except for thermocouples which located at axial stations in the vicinity of secondary air, there is little deviation between the measured and radiation corrected temperatures. This may be due to the fact that for a given gas temperature, the errors are very sensitive to the wall temperature.
- In general this study indicates that radiative corrections to thermocouple data (in this laboratory scale combustor) can be negligible.
- It also appears the presence of the deflector dampens the difference from applying both methods of radiative correction (bare bead versus single shielded aspirated) over the combustor. This may be due to the deflector causing more uniformity in the temperatures between the centreline and wall particularly in the downstream.

7.1.2 Deflector effects in combusting packed beds

A laboratory scale combustor with continuous feeding system used to characterize the influence of deflectors on combustion performance. A specially designed deflector with an adjustable rod allowed regulating the deflector at different axial position. Fifteen thermocouples were used to ascertain the axial and radial temperature distributions and gaseous emissions (O_2, CO, CO_2 and NO) were monitored by a continuous sampling gas analyser, the following conclusions have been drawn:

- Using a deflector generally reduces the level of NO emissions but leads to a rise in the average CO emissions. Varying the location of deflector in the freeboard appears to influence CO, whilst NO emissions are not sensitive to

the location of the deflectors. In addition, results show that deflectors don't have appreciable impact on the burning rate.

- The presence of a deflector appears to increase the near-wall temperature profiles upstream of the secondary air, but decrease near-wall temperatures in the downstream.
- It is believed the effects of the deflectors appear to be due to change the fluid flow upstream of the deflectors through longer residence time.

7.1.3 Effect of freeboard deflectors on the exergy in combusting packed beds

The influence of deflectors on the exergy analysis in a fixed bed biomass combustor has been studied. This study includes experiments conducted on continues feed pellet combustor, with a freeboard deflector located at different axial locations, the following conclusions can be drawn:

- CO chemical exergy and total exergy decrease when the air-fuel equivalence ratio (λ) increases.
- Mechanical exergy is sensitive to the axial position of the deflector (H). By raising the deflector position, it more significantly affects the mechanical exergy in the downstream.
- In general this study indicates that the deflectors do not have significant impact on the total exergy and CO chemical exergy of the flue gases at the exhaust section.
- An uncertainty analysis has been applied to a sample number of text cases, whereby the likely ±3% variation on temperature, CO emissions as well as exergies has been estimated

7.1.4 Deflector effects in non-combusting packed beds

A commercial CFD software package ANSYS Fluent (version 14.5) was used to simulate heat transfer and fluid flow inside a packed bed and freeboard by implementation of a three-dimensional CFD model of a porous media. Furthermore, MATLAB (ver. 2012b) codes have been developed to post-process the combustion variables, extracting steady state time period and establish the radiation corrected temperature for thermocouples. An overall summary of the results is given below.

- For the temperature range investigated (100°C to 400°C), the numerical results reveal that deflectors influence the temperature distributions in the freeboard by increasing the wall temperature but this depends on the mode of heating (wall heated versus heated primary air).
- The impact of deflectors on the temperature profiles inside the non-reactive packed bed (below the freeboard) has been found to be negligible. By changing the boundary conditions and increasing inlet air temperature (instead of constant wall temperature), the deflector more significantly affects both the temperature distributions inside the packed bed column.

7.2 Future work recommendations

- Investigating the effect of freeboard deflectors on particulate emissions over the range λ_{Total}=1-3 (experimental work).
- Investigating the effect of freeboard deflectors in different air staging strategies (ratio of secondary/primary air) on the emissions and temperatures (experimental work).
- Whereas the present study has used a square shaped deflector, a future research project using different deflector with different shapes (and dimensions) may investigate the effects of deflector shape on the combustor performance (experimental work).
- Further works are required to optimize the secondary air flow rate and minimize emissions in the presence of a deflector (experimental work).
- More work is warranted to further identify the role of freeboard deflectors at higher inlet air temperature or where the heat source occurs at the top of the non-reactive packed beds (numerical work).
- Develop a complete combustion model (including emissions) for simulation of freeboard deflectors in fixed bed combustors (numerical work).
- Simulation of non-reactive packed bed by implementation of the radiative heat transfer between two phases in the porous media, as it is of key importance at higher temperatures (T>800^{o}C) (numerical work).
- Computational based studies to develop a model for simulation of deflector effects in an industrial combustors to optimise combustion process (numerical work).

- A wider experimental testing campaign, featuring multiple repetitions of similarly operated combustor test conditions as well as broader stoichiometry and error analyses, is warranted so as to more generally analyse the effects of freeboard deflectors.

Appendices

Appendix A Permission of copyrighted material

Please refer to the attached CD (CD-1) for the permissions of published article to use in the thesis.

Appendix B Statement of co-authors contribution

Please refer to the attached CD (CD-2) for detailed documents of statement of co-authors contribution for each publication listed.

Appendix C Mathematical modelling

C-1 Classification of the packed bed combustion models

To date various models have been developed and introduced to simulate combustion in packed beds. The selection of suitable governing equations is an important step which affects the solution [1] and it is also use useful to categorize the solutions according to the scale of modelling the bed. In this regard, a packed bed can be treated as a continues porous medium if intra-particle effects are fairly negligible. However, if the bed consists of rather large fuel particles, then assuming a continuous bed will produce inaccurate results because of considerable intra-particle gradients. When the Biot number Bi>>1, temperature gradients will exist inside fuel particles and the size of pellets fuel cannot be neglected [2-4]. A summary of fix-bed combustion models according to the scale of modelling can be classified as following:

Microscale models: This model has been developed for in depth studies of heat and mass transfer as well as simulations of the reactions inside single particle [4]. Moreover, by using this scale of modelling, effects of free water inside a particle (moisture) can also be studied as shown in Figure C-1.

Macroscale models: These models assume the bed to be an integrated porous medium consisting of gas and solid phases and combustion is simulated through the whole fuel bed. This approach is acceptable for thermally thin solid particles[1] [5] as shown in Figure C-2.

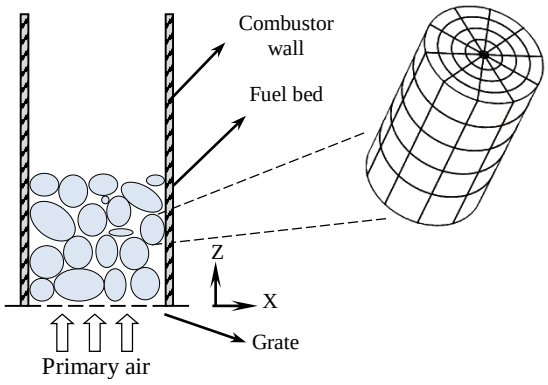

Figure C-1 Microscale model which consider simulation of the single solid particle.

[1] Temperature difference across the particle is negligible.

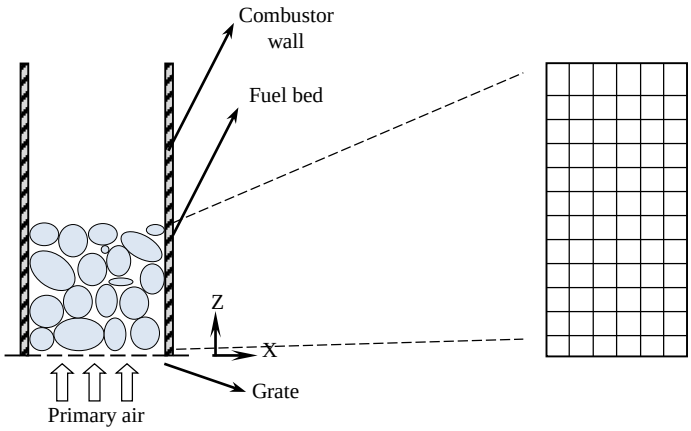

Figure C-2 Macroscale model consider the entire bed as an integrated porous medium.

Particle-resolved macroscale models: This modelling approach is a combination of the two previous models. The solid phase is assumed as a finite number of fuel particles, which one individually described by microscale models. Additionally, the packed bed is simulated by a macroscale model and boundary conditions are used to connect the particle model with the macroscale model. Figure C-3 shows a typical mesh of particle-resolved macroscale model [6].

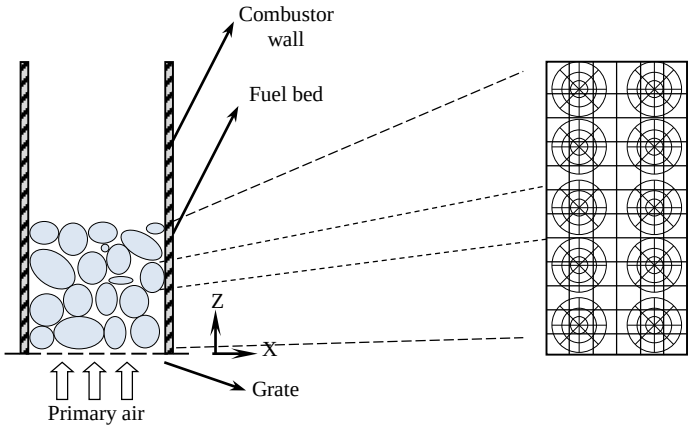

Figure C-3 A particle-resolved macroscale model.

C-2 General governing equation

Combustion reaction process consists of various types of physical and chemical phenomena. Conservation laws of mass, momentum and energy govern combustion

processes. A system of transient partial differential equations is employed to represent these phenomena. In a general form, the following equation describes a bed model in the unsteady situation [7]:

$$\frac{\partial(\varepsilon\rho\phi)}{\partial t} + \nabla.(\varepsilon\rho v) = \nabla.(\Gamma\nabla\phi) + S_\phi \quad \text{(C.1)}$$

$\frac{\partial(\varepsilon\rho\phi)}{\partial t}$: Unsteady term

$\nabla.(\varepsilon\rho v)$: Convection term

$\nabla.(\Gamma\nabla\phi)$: Diffusion term

S_ϕ: Source term

where ε is porosity, ρ(kg/m^3) is density, v (m/s) is a vector of interstitial velocity[1], ϕ is transported (scalar) quantity, Γ is diffusion coefficient and $S\varphi$ includes all source terms. The product $\varepsilon\rho$ is called bulk density. By substitution ϕ, Γ and S_ϕ with certain physical quantities, equation (C.1) becomes a governing equation for heat, mass or momentum transfer. Source term of equation (C.1) consists of whatever which cannot be fitted into the unsteady, convection or diffusion terms. For the energy equation, heat transfer rates always include convective heat transfer and heat release or consumption of chemical reactions. For calculation the radiation heat transfer usually a separate system of ordinary differential equations are employed and the radiation heat flux enters the energy transport equation through the source term [8, 9]. Also the radiation effects can be lumped into the effective thermal conductivity [10].

Table C-1 shows some of the physical quantities which are commonly met in the fuel bed models. In heterogeneous model mass and heat transfer are described by distinguished equation for each phase. Conversely in homogenous model, temperature and mass concentration gradients at the fuel particle are insignificant (usually in fine particles) and the model can be further simplified to a one-phase model [11]. In addition to the description of the coefficients, various modelling can be used to develop different form of the governing equation. For example, Yang et al. [12] developed 1D model which use the momentum equation to solve gas flow,

[1] Interstitial velocity is a measurement of how fast fluid flows through a medium in a particular direction.

while other 1D models calculated the gas flow direct from the continuity equation [10, 13]. These models assume a plug flow in the combustor with constant pressure.

Table C-1 Coefficients of the general governing equation with related physical units for transport equations in fuel bed models [6].

Equation	φ	Γ	S_φ
Continuity	1	0	Sum of heterogeneous reaction rates r
Species	Mass fractions Product of i-th species Y_i	Product of bulk density and effective mass dispersion coefficient $\varepsilon\rho D_i$	Rate of production or consumption of species r_i
Energy	Specific enthalpy h	Product of bulk density and effective mass dispersion coefficient λ/C_p	Heat transfer rate $\dot{q}$
Momentum	Velocities v_j	Dynamic viscosity $\varepsilon\mu$	Pressure gradient ∇P, gravity force, interphase momentum transfer f

C-3 Pressure drop

The Ergun equation expresses pressure drop due to resistance of the bed. This equation shows how friction factor in a packed column and the Reynolds number are related [14]:

$$f_p = \frac{150}{Re_p} + 1.75 \tag{C.2}$$

where f_p and Re_p are defined as:

$$f_p = \frac{\Delta p}{L}\frac{D_p}{\rho V_s^2}\left(\frac{\varepsilon^3}{1-\varepsilon}\right) \tag{C.3}$$

$$Re_p = \frac{D_p V_s \rho}{(1-\varepsilon)\mu} \tag{C.4}$$

Where Δp is the pressure drop across the bed, L is the bed height, D_p is the equivalent spherical diameter of the packing, ρ is the flowing gas density, μ is the dynamic viscosity of the flowing gas, V_s is the superficial velocity (i.e. gas velocity through an empty tube at the same volumetric flow rate) and ε is the bed porosity.

C-4 Modeling of the combustion sub-processes

In this regard, combustion process is divided into four major steps: moisture evaporation (fuel drying), pyrolysis, gasification and combustion (high temperature oxidation reactions).

C-4.1 Models of moisture evaporation

The drying models can be categorized into three different types [15]:

Heat sink model: The basis of this model is that drying occurs at a fixed saturation temperature and the drying region is infinitely thin and behaves same as a heat sink. Water vapour leaves the particle at once because there is no resistance to mass transfer and the drying rate is controlled by heat transfer [16].

First-order kinetic rate mode: In this model a first order kinetic equation is employed to simulate the evaporation rate with drying depending on temperature and moisture content of the fuel particle. This model is expressed by an Arhenius-type expression:

$$r_{dry} = Aexp\left(-\frac{E_a}{RT_s}\right)\rho_{sb}Y_{H_2O,s} \quad \text{(C.5)}$$

Where r_{dry} is the rate of drying (kg/m^{3}s), A (1/s) is pre-exponential factor, E_a (J/mol) is the activation energy, R (J/mol K) is the universal gas constant for the coflowing air, T_s (K) and ρ_{sb} (kg/m3) are solid phase temperature and bulk density, respectively, and $Y_{H2O,s}$ (kg/kg) is mass fraction of water contained in the fuel.

Equilibrium model: Is based on the assumption that water vapour is in equilibrium with the coflowing gas. As a result the saturation pressure will be fixed the partial pressure of water vapour. This hypothesis is conventional for low-temperature drying. Equilibrium models are dependent on both the heat transfer and the mass transfer and governed by:

$$r_{dry} = k_d A_p(\rho_{sb})\rho_{H_2O,surf} - \rho_{H_2O,g} \quad \text{(C.6)}$$

Where k_d (m/s) is mass transfer coefficient, A_p (m^2/m^3) is volumetric particle surface area and $\rho_{H2O,surf}$, $\rho_{H2O,g}$ (kg/m^3) are densities of water vapour at particle surface and in the gas phase, respectively [9, 17].

C-4.2 Model of pyrolysis

Biomass generally contains large proportion of volatile content and a smaller amount of low char content, which makes biomass a highly reactive fuel. However, the volatile content varies for different biomass fuels, which subsequently influences the thermal behaviour of the fuel. When the fuel is heated up to a certain temperature, volatile matter is gradually released in gaseous phase after moisture evaporation first acts as a heat sink. If the temperature is raised further, the solid fuel is thermally decomposed as external oxidizing species cannot penetrate into particle pores due to the flow of released volatiles. In this content, the devolatilization is also referred to as pyrolysis. If there is enough surrounding oxygen, these released gaseous volatiles burn again when temperature exceeds a certain level.

It is often assumed that devolatilization is almost neutral with respect to heat release or consumption [18]. With this process in mind, a one- step global reaction can be used to describe the devolatilization of solid fuels [19] and a first-order kinetic rate model is employed to describe he pyrolysis rate r_{pyr}:

$$Fuel \rightarrow Volatiles + Char \tag{C.7}$$

$$r_{pyr} = Aexp\left(-\frac{E_a}{RT_s}\right)\rho_{sb}Y_{vol,s} \tag{C.8}$$

where Y_v is the mass fraction of volatile matter in the fuel particle [20].

C-4.3 Combustion reaction model

Gaseous products, which are released through the pyrolysis process, mix together with the combustion air before homogenous reactions can take place. After that, chemical kinetics control the process in the gas phase. These reaction rates can be estimated by taking the minimum of the mixing rate and chemical kinetics rate as obtained from an Arhenius-type expression. In practical operation, a fuel-rich combustion mode occurs in the bed if excessive amounts of unburnt volatile gases leave the bed, and inadequate air is injected into the combustor. Under those

conditions, modelling of the reactions can be assumed as a freeboard model. In this case a commercial CFD packages with more detailed reaction schemes such as ANSYS FLUENT can be employed [19].

After pyrolysis, emissions of volatile gas stop, so external oxidizing agents can diffuse through the boundary layer of a solid particle and react with the remaining carbon. Char oxidization is described by [19]:

$$C+\alpha O_2 \rightarrow 2(1-\alpha)CO+(2\alpha-1)CO_2 \quad \text{(C.9)}$$

where α is determined from product formation ratio r_{CO}/r_{CO2}, which depends on the fuel temperature and is usually expressed as [10]:

$$\frac{r_{CO}}{r_{CO_2}} = Aexp\left(-\frac{E_a}{RT_s}\right) \quad \text{(C.10)}$$

The rate of char oxidation is a function of the kinetic reaction rate and the rate of oxygen diffusion to the particle surface and the rate of char oxidation is generally expressed as [6]:

$$r_c = A_p \frac{k_C k_D}{k_C + k_D} P_{O_2} \quad \text{(C.11)}$$

where A_p (m^2/m^3) is volumetric surface of the particle, k_c (kg/m^2 s Atm) is Arhenius-type kinetic rate constant, k_D (kg/m^2 s atm) is coefficient of mass transfer and P_{O2} (atm) is partial pressure of oxygen in gas phase. Yang et al. [19] and Zhou et al. [10] reported the parameters needed for the reaction modelling. The kinetics for wood pellet combustion in the current project will be derived using literatures [19, 21].

C-5 Radiation heat transfer

Radiative heat transfer from the walls and from the flame in the combustor affects solid fuel dying, devolatilization, and combustion and included through the source term in the energy equation (C.1), S_ϕ.

$$S_\phi = -\nabla . q(\vec{r}) = -\int_0^\infty \int_0^{4\pi} \frac{dI_\lambda}{ds} \partial\Omega \, \partial\lambda \quad \text{(C.12)}$$

Where $q(\vec{r})$ is radiative heat flux vector (W/m), $\vec{r}$ is position vector (m), s is coordinate along the path of a radiation ray (m), and I_λ is intensity of radiation at the wave length λ (W/m^2 sr μm).

Additionally Radiation Transfer Equation (RTE) for an absorbing, emitting and scattering medium expressed as:

$$\frac{dI_\lambda}{ds} = \hat{s}.\nabla I_\lambda = -\kappa_\lambda I_\lambda(\vec{r},\hat{s}) - \sigma_{s,\lambda} I_\lambda(\vec{r},\hat{s}) + \kappa_\lambda I_{b,\lambda}(\vec{r}) + \frac{\sigma_{s,\lambda}}{4\pi}\int_0^{4\pi} I_\lambda(\vec{r},\hat{s}_i)\Phi_\lambda(\hat{s}_i,\hat{s})\partial\Omega_i \qquad \text{(C.13)}$$

where λ is wavelength (μm), κ is absorption coefficient, σ_s is scattering coefficient, I_b is black body radiation, Ω_i is solid angle in s direction (sr), Φ is scattering phase function, $\vec{r}$ is position vector, and $\hat{s}$ is direction vector, Figure C-4 can be used to explain the terms of RTE equation over a finite volume, whereby it depicts a radiation beam travelling (along direction s) in an absorbing, emitting and scattering media. As the beam passes through the medium, some energy is lost from the beam due to absorption and scattering in the media. In addition, the beam may gain energy from incoming scattering and gas emission emitted from the media. In equation (C.13), the first two terms on the right hand side represent losses due to absorption and scattering whereas the last two terms stand for gains due to energy emitted from the media and incoming scattering [22].

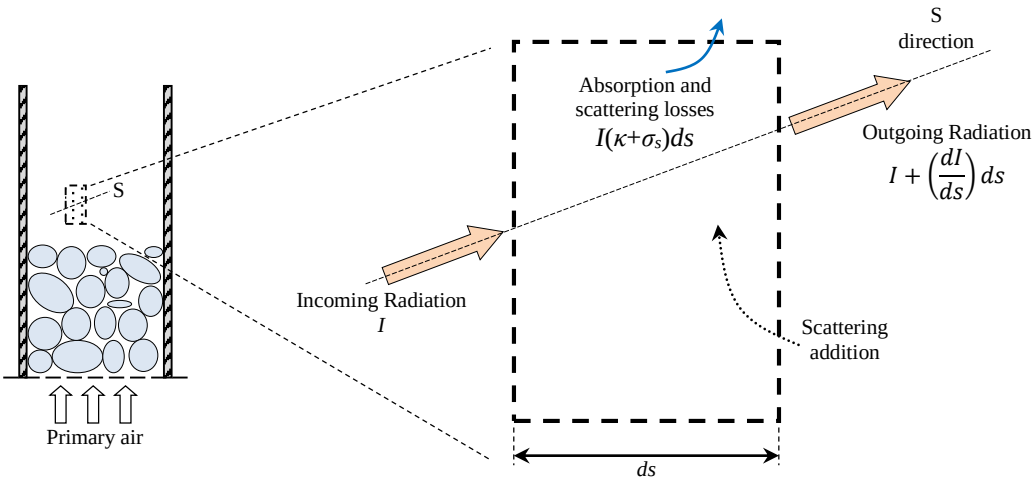

Figure C-4 Modeling of radiation heat transfer.

Simplifications need to be done to help solve the RTE equation and several numerical methods have been developed to solve it. The most important approaches are Optically Thin model (OT), P1-approximation model and Finite Volume Method (FVM) [23].

C-6 Heat loss from the combustor wall

Combustor wall temperature affects combustion performance. Heat transfer rate from a reactor wall (to the environment) has significant effect on the wall temperature and reducing this heat loss more heat will be available for the various stages of combustion to take place. A rate of heat transfer balance is a primary tool for estimating the heat loss from the combustor wall to the environment. In this regard, there are two general approaches to establishing heat balance: heat balance in terms of temperature and in terms of enthalpy.

Heat balance with respect to the temperature: Figure C-5 shows heat fluxes in a combustor, a source term can be defined as following:

$$\dot{q}_1 - \dot{q}_2 - \dot{q}_3 + S = 0 \tag{C.14}$$

where q_1 is the heat flow of incoming air (J/s), q_2 is heat lost to the environment via combustor walls, q_3 is the heat taken up by flue gases and S heat (source term) generated by the reaction front. The heat fluxes and the source term are defined as:

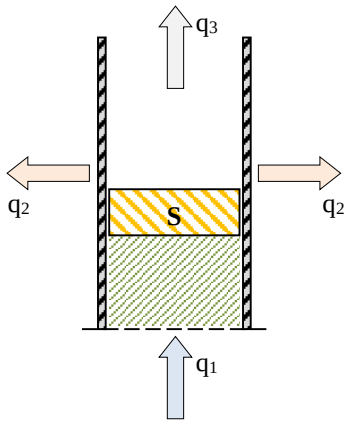

Figure C-5 Heat fluxes.

$$\dot{q}_1 = \dot{m}_{in} C_{p,in} T_{in} \pi R^2 \tag{C.15}$$

$$\dot{q_2} = -\int_0^L h(T_i - T_e)2\pi R dl \quad \text{(C.16)}$$

$$\dot{q_3} = \dot{m_{out}} C_{p,out} T_{out} \pi R^2 \quad \text{(C.17)}$$

$$S = \dot{m}_s Q \pi R^2 \quad \text{(C.18)}$$

where $\dot{m_{in}}$is the mass flux of the incoming air (kg/m^2 s), $C_{p,in}$ is the specific heat capacity (J/kg K), T_{in} is the in inlet air temperature (K), R is the radius of reactor (m), h is the convection heat transfer coefficient (W/m^2 K), T_i is the inner wall temperature, T_e is the outer wall temperature, l is the length of the reactor tube, $\dot{m_{out}}$ is the mass flux of product gases, T_{out} is the outlet temperature of product gasses, $\dot{m}_s$ is the solid fuel mass flux, and Q is the heat of the reaction (J/kg). The assumptions for the heat balance are:

- For the estimation of the heat of reaction, it is assumed that the fuel burnt completely.
- Specific heats are averaged over the cross section of the combustor tube.
- The heat transport through the combustor wall can be described with heat transfer coefficient.

Heat balance in terms of the enthalpy: Heat balance with respect to the enthalpy expressed as:

$$\dot{h_1} + \dot{q_2} + \dot{h_3} = 0 \quad \text{(C.19)}$$

$$\dot{h_1} = \sum h_{i,in} Y_{i,in} \dot{m_{in}} \pi R^2 \quad \text{(C.20)}$$

$$\dot{q_2} = -\int_0^L h(T_i - T_e)2\pi R dl \quad \text{(C.21)}$$

$$\dot{h_3} = \sum h_{i,out} Y_{i,out} \dot{m_{out}} \pi R^2 \quad \text{(C.22)}$$

where h_i is the specific enthalpy (Jkg^{-1}), $\dot{h_1}$ is the heat flow (Js^{-1}), and Y_i is the mass fraction of the gaseous species The species Y_i can be determined by using gas analysis tools such as gas chromatography.

Appendix D MATLAB Codes

D-1 Percentile mean deviation

This code is used to calculate percentile mean deviation over different time windows for temperatures and emissions data (Chapter 2, Figure 2.6 and 2.8)

D-2 The relative significance of radiative corrections

This code used to ascertain the radiative corrections to thermocouples data for each experimental test (Chapter 2, Figures 2.10 and 2.11).

D-3 Estimation the deviation of raw data

This code used to estimate the deviation of the experimental data (Chapter 2, Figures 2.1).

D-4 Determine the steady state temperatures and emissions data

This code is used to analyse the temperatures and emissions data. This program determines the average value of combustion parameters for the steady state time period and save data for the selected tests in Excel files. The code was mainly used to assess the effects of deflector on temperatures and emissions (Chapter 3).

D-5 Determine the flue gases availability

This code is used to estimate the exergy of the combustion gases at the exhaust section (Chapter 5).

D-6 Mechanical exergy at Determine the flue gases availability

This code is used to estimate the mechanical exergy at different axial locations (Chapter 5).

Please refer to the attached CD (CD-3) for MATLAB source codes.

Appendix E Experimental setup and methodology

The experiments were conducted on a laboratory scale combustor located at the University of Vigo, Spain. Details can be found in Chapter 2 and 3.

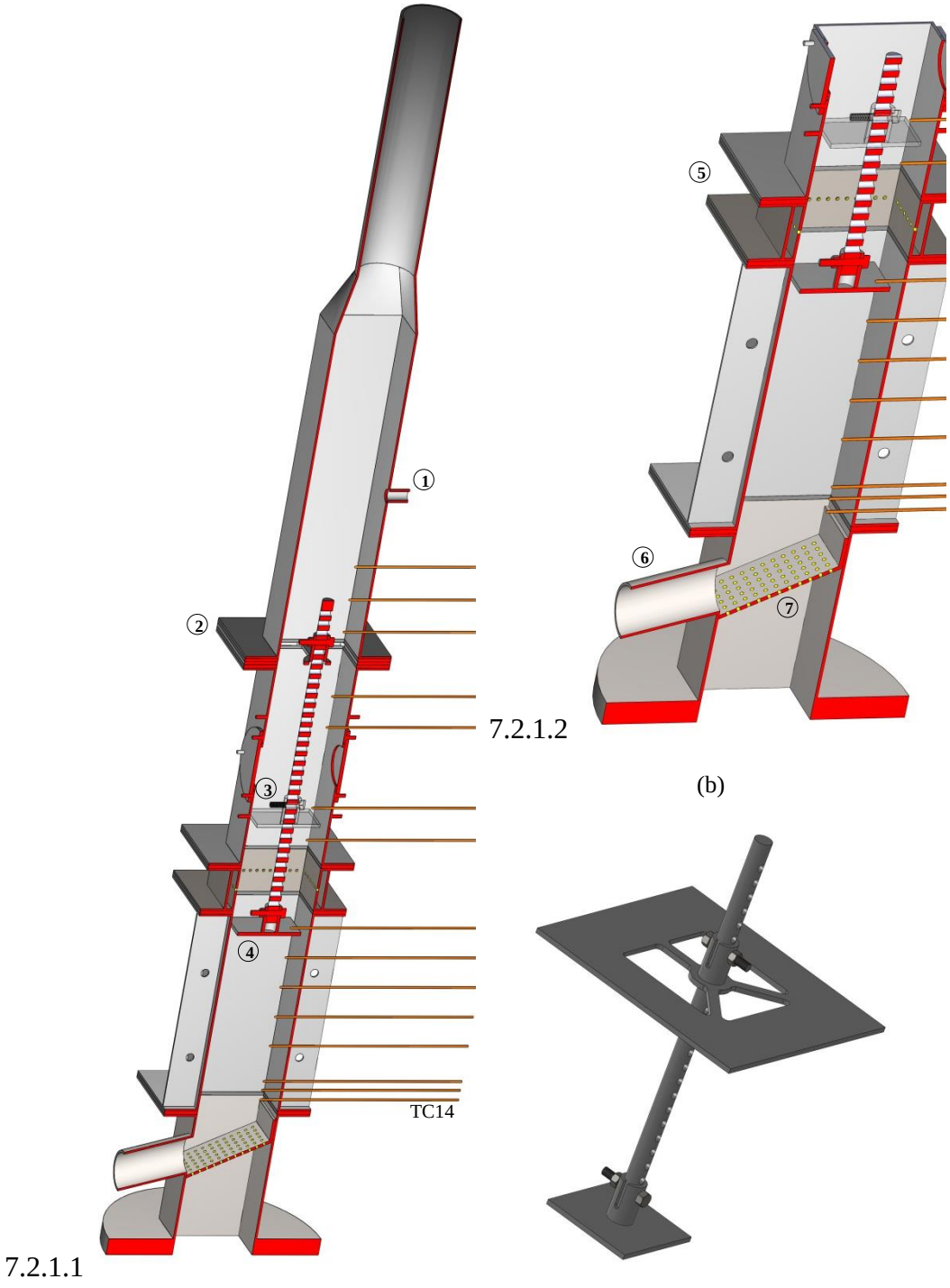

(1) Emission measurment port, (2) Deflector holder, (3,4) Deflector at two different axial positions, (5) Secondary air, (6) Primary air, (7) Grate

Figure E-1 (a,b) CAD generated cross sections of the experimental setup showing relevant components; (c) Deflector and deflector holder .

(a) (b)

Figure E-2 (a) pellet fuel feeding unit; (b) pellet fuel; (c) Fuel bed and thermocoples (TC14-TC13).

(a) (b)

Figure E-3 Primary air section (a) before installing the removable viewing window at the beginning of test; (b) viewing window is reattached.

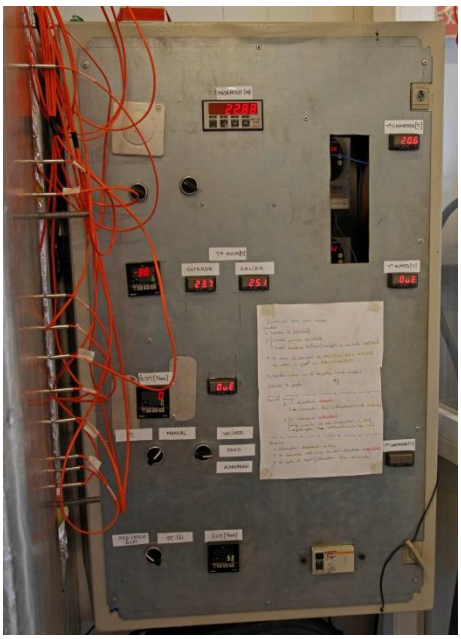

(a)

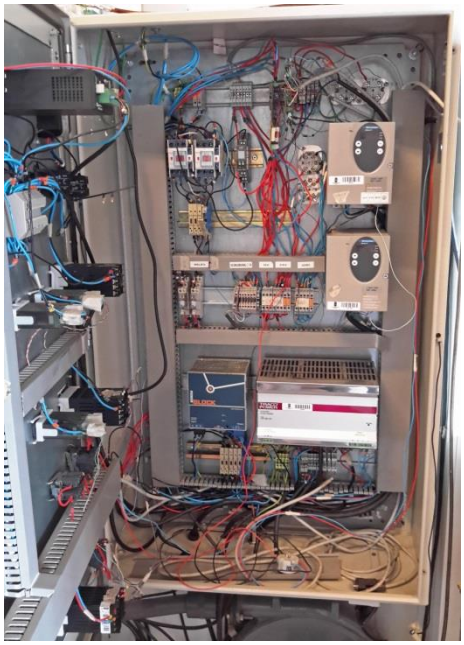

(b)

(c)

(d)

Figure E-3 (a,b) Control box; (c) Gas analyser (make: Servomex model: Servopro 4900); (d) Gas conditioner (make: JCT, model: JCC).

Please refer to the attached CD-4, CD-5 and CD-6 for details of the experimental rig and data sets.

E-1 Methodology

E-1.1 Experimental methodology

The modular (laboratory scale) fixed bed combustor incorporates four main (modular) sections: I- Plenum, II- Primary section, III- Secondary section, and IV- Exhaust (Figure 2.1a). The chamber is made of 310 stainless steel (6mm thick) and has a 120mm×120mm square cross section and overall height of 1500mm. The walls are left uninsulated and left in free contact with ambient air to prevent

overheating. The primary air (Q_p) enters the bed from beneath (via a side port) and through the plenum section and grate. The grate helps promote a more homogeneous distribution of inlet air and carries the fuel pellets. The grate is positioned with a 25 degree gradient (Figure 3.2c) to help the fuel pellets move and avoid crushing the wood pellets which are fed upwards by a screw feeder system. Primary air is supplied by a variable frequency drive centrifugal fan coupled to a digital controller in order to maintain a constant airflow. The primary air flowrate is measured by an in-line mass airflow sensor.

Nominal characteristics the biomass fuel (wood pellet) that is used in this study are presented in Table 2.1. The wood pellets have uniform size and shape with a diameter of 6mm and length of 20mm (Figure 2.1b). The continuous feeding unit includes hopper and screw conveyor. The screw conveyor system delivers pellet fuel from the hopper and fed upwards towards the inclined grate. The mass flow of wood pellets into the combustor is controlled by an adjustable on-off digital timer. The hopper is suspended from a weighing system that features a tensile load cell so as to monitor the weight loss of the pellet fuel.

The combustor includes a secondary air section (Figure 3.2d) which introduces air (Qs) via 44 uniformly distributed holes (φ=4mm). The secondary air is controlled by a separate centrifugal fan drive and another mass flow meter is used to measure the secondary air flow rate. The exhaust section is placed above the secondary air section and has an overall height of 1300mm. The exhaust is diluted with ambient air so as to cool the flue gases before passing into the chimney. The square shaped stainless steel deflector (95mm×95mm) is attached to an adjustable rod which can be used to regulate the deflector axial position.

To determine the temperature profiles across combustor sections, fifteen thermocouples (outer diameter of 3mm) penetrate through access ports on the combustor side wall (Figures 3.2a and 2.1a). The thermocouples can be positioned at different radial positions. Thermocouples used for measurements are Type N, sheathed and having a temperature range between -270°C to 1300°C. Thermocouples data were fed to the data acquisition system by a 16-Channel thermocouple input module. Thermocouples TC0 to TC6 were used to determine

the downstream temperature profiles whilst thermocouples TC7 to TC14 measure upstream temperatures in section-II.

To monitor gaseous emissions (O_2, CO, CO_2, NO) a continuous sampling gas analyser were used. This system consists of two major units: a gas conditioning system and a continuous sampling gas analyser. Gaseous emissions are withdrawn using a port located at x=110mm from the uppermost thermocouple position TC0. A continuous sample is obtained by a suction probe, passed through a heated line and fed into a gas conditioning system to avoid water vapour cross sensitivities and volumetric errors. After these treatments stages the flue gas sample is finally introduced into the continuous gas analyser. To generate a time series of temperatures and emissions, all data is streamed real-time to a computer using a LabView interface (Ver. 2014).

E-1.2 Numerical approach

To investigate the effects of deflectors on the heat transfer inside non-reactive packed beds, ANSYS Fluent (version 14.5) was applied to resolve fluid dynamics and heat transfer. A three-dimensional Computational Fluid Dynamics (CFD) model of a porous media is adopted to model the influences of freeboard deflector on packed bed columns through the utilisation of suitable effective thermal conductivity values based on published empirical models. The equations governing the transport of mass, momentum and energy for a porous media can be found in Chapter 5. In this research, the surface-to-surface (S2S) model has been used to account for radiation exchange in the CFD simulations.

To facilitate data analysis MATLAB (ver. 2012b) codes have been developed to post-process the combustion variables. These programs were used to read through all the combustion data in Excel spreadsheets, process data, extract steady state time period, evaluate the radiation error of thermocouples and estimate flow availability for each test. Appendix D present the entire m-file of the MATLAB programs.

Appendix F Uncertainty analysis

Every measurement is subject to some uncertainty. Measurement errors can come from the measuring instrument such as thermocouple and gas analyser, from the operator, from the environment and from other sources. This section presents an overview of the uncertainty analysis theory and the derived uncertainties for emissions and temperatures data.

F-1 General theory

All experimental uncertainty is due to either random errors or systematic errors [24-26]:

$$\varepsilon_{Total} = \pm\sqrt{\varepsilon_s^2 + \varepsilon_r^2} \quad \text{(F.1)}$$

where, ε_{Total} is the total uncertainty, ε_s is the systematic error and ε_r is the random error. Systematic errors in experimental observations usually come from the measuring instrument limits (i.e. the accuracy of measurement device). Whilst random errors are statistical fluctuations in the measured data which caused by unknown and unpredictable changes in the experiment. These changes may occur in the measuring instruments or in the environmental conditions[25].

$$\varepsilon_s = \sqrt{\sum_{i=1}^{n} \varepsilon_{s,i}^2} \quad \text{(F.2)}$$

$$\varepsilon_r = \sqrt{\sum_{i=1}^{n} \varepsilon_{r,i}^2} \quad \text{(F.3)}$$

where, n is the number of error source. The individual component of the random error in Equation (F.3) is calculated as:

$$\varepsilon_{r,i} = \sqrt{\frac{\sum_{i=1}^{N}(\phi_i - \bar{\phi})^2}{N(N-1)}} = \frac{\sigma_s}{\sqrt{N}} \quad \text{(F.4)}$$

$$\bar{\phi} = \frac{1}{N}\sum_{i=1}^{N} \phi_i \quad \text{(F.5)}$$

where, σ_s is the standard deviation of a sample mean, $\bar{\phi}$ is the mean of a measured parameter and N is the number of samples in the repeated observations.

F-2 Systematic uncertainties

Uncertainties in temperature and emission measurements are mainly associated with the accuracy of the thermocouples and gas analyser. Thermocouples used for measurements are Type N, (make: TC measurement, model: 2I-Nickel-Silicon-Magnesium) and have an outer diameter of 3mm and sheath length of 300mm. These thermocouples are rated over a temperature range of -270°C to 1300°C. Within this range the temperature data acquisition system has an accuracy of 0.4% [27]. A continuous sampling gas analyser (make: Servomex, model: SERVOPRO 4900) is used to monitor fire species (O_2, CO, CO_2, NO) in the flue gas. Table F-1 presents the accuracy of the gas analyser [28].

Table F-1 Accuracy of the gas analyser.

Gas	Accuracy
O_2	0.01%
CO	1%
CO_2	1%
NO	1%

F-3 Random uncertainty

Random errors can be reliably estimated by repeating measurements. Table 4.3 shows the operating conditions for tests. These tests have been banded into three ranges of stoichiometry (λ). Measured data from tests 32, 33 and 34 have been chosen to estimate the random errors. These test share same operating conditions (Q_p, Q_s) and have similar combustion stoichiometry ($0.43 < \lambda < 0.51$). Table F-2 shows the average values of thermocouples and gas species data extracted over the steady state period for the selected tests (Chapter 4).

F-4 Results

The total, systematic and random uncertainty values for the temperatures and emissions are derived using Equations (F.1), (F.2) and (F.3), respectively. The results are presented in Table F-3. Table F-4 presents the uncertainty values of the chemical exergy, CO exergy and total exergy.

Table F-2 Steady state values of temperatures and emissions for the selected tests.

		Test 32	Test 33	Test 34
	Q_p (l/min)	60	60	60
	Q_s (l/min)	240	240	240
	Deflector Position, H (mm)	240	240	240
	Thermocouple position, r (mm)	5	5	5
Temperature (ºC)	**TC0**	229.461	239.696	198.075
	TC1	264.932	282.338	228.245
	TC2	254.252	271.090	219.128
	TC3	273.605	278.596	227.167
	TC4	282.109	287.914	233.783
	TC5	294.271	309.605	250.093
	TC6	314.590	347.011	268.958
	TC7	519.970	506.943	506.456
	TC8	445.363	432.517	460.959
	TC9	460.501	432.494	477.918
	TC10	460.939	412.158	479.803
	TC11	480.386	419.533	503.755
	TC12	555.232	509.101	568.176
	TC13	490.465	419.734	451.352
	TC14	510.844	475.846	526.413
Emissions	**NO (vpm)**	52.848	54.247	50.878
	O_2 (%)	14.909	14.443	15.048
	CO (%)	1.391	1.461	1.566
	CO_2 (%)	8.696	8.718	8.611

Table F-3 Systematic, random and total uncertainty of measured parameters.

	Parameter	Systematic uncertainty (±%)	Random uncertainty (±%)	Total uncertainty (±%)
Temperature (ºC)	**TC0**	0.4	4.60	4.61
	TC1	0.4	5.03	5.05
	TC2	0.4	5.04	5.05
	TC3	0.4	5.15	5.16
	TC4	0.4	5.23	5.24
	TC5	0.4	5.12	5.13
	TC6	0.4	5.96	5.97
	TC7	0.4	0.71	0.81
	TC8	0.4	1.50	1.56
	TC9	0.4	2.36	2.40
	TC10	0.4	3.65	3.67
	TC11	0.4	4.38	4.40
	TC12	0.4	2.69	2.72
	TC13	0.4	3.68	3.70
	TC14	0.4	2.42	2.45
Emissions	**NO**	1	1.51	1.82
	O_2	0.01	1.01	1.01
	CO	1	2.82	2.99
	CO_2	1	0.31	1.05

Table F-4 Uncertainty values of chemical exergy, CO exergy and total exergy.

Parameter	Systematic uncertainty (±%)	Random uncertainty (±%)	Total uncertainty (±%)
Chemical exergy	1.00	1.89	2.14
CO exergy	0.4	1.36	1.69
Total exergy	1.78	1.58	2.38

Appendix G Supplementary materials

Following datasets and combustor design are included in the attached CD of the thesis.

i. MATLAB code for combustion data processing and calculating the percentile mean deviation (CD-3).
ii. MATLAB code used to ascertain the radiative corrections to thermocouples data (CD-3).
iii. MATLAB code for calculating the deviation of raw data (CD-3).
iv. MATLAB code for determining the steady state temperatures and emissions data (CD-3).
v. MATLAB code for calculating the exhaust gases exergy (CD-3).
vi. MATLAB code for calculating the mechanical exergy along the combustor (CD-3).
vii. Combustor design files (CD-4).
viii. Datasets of the experimental tests (CD-5)
ix. Photos of the experimental rig (CD-6).

Appendix References

1. Van Kuijk, H.A.J.A., *Grate furnace combustion: A model for the solid fuel layer.* PhD Thesis, Eindhoven University of Technology, 2008: p. 69-78.
2. Incropera, F.P., and Dewitt, D. P. , *Fundamentals of Heat and Mass Transfer, 5th ed.* John Wiley & Sons, New Jersey, USA, 2002.
3. Yang, Y.B., Ryu, C., Khor, A., Sharifi, V. N., and Swithenbank, J., *Fuel size effect on pinewood combustion in a packed bed.* Fuel, 2005. 84: p. 2026–2038.
4. Yang, Y.B., Sharifi,V. N., Swithenbank, J., Ma, L., Darvell, L. I., Jones, M., Pourkashanian, M., and Williams, A., *Combustion of a single particle of biomass.* Energy and Fuels, 2008. 22: p. 306-316.
5. B. Benkoussas, J.L.C., B. Porterie, N. Sardoyb, J. C. Loraud, *Modelling thermal degradation of woody fuel particles.* International Journal of Thermal Sciences, 2007. 46: p. 319-327.
6. Jurena, T., *Numerical modelling of grate combustion.* PhD Thesis, Brno University of Technology, Faculty of Mechanical Engineering, 2012.
7. Yin, C., Rosendahl, L. A., and Kaer, S. K. , *Grate-firing of biomass for heat and power production.* Progress in Energy and Combustion Science, 2008. 34(6): p. 725-754.
8. Ryu, C., Shin, D., and Choi, S., *Combined simulation of combustion and gas flow in a grate-type incinerator.* Journal of the Air & Waste Management Association, 2002. 52: p. 174-185.
9. Yang, Y.B., Goh, Y. R., Zakaria, R., Nasserzadeh, V., and Swithenbank, J., *Mathematical modelling of MSW incineration on a travelling bed.* Waste Management, 2002. 22(4): p. 369-380.
10. Zhou, H., *Numerical modelling of straw combuster in a fixed Bed.* Fuel, 2004. 84: p. 389-403.
11. Thunman, H., and Leckner, B., *Influence of size and density of fuel on combustion in a packed bed.* Proceedings of the Combustion Institute, 2005. 30: p. 2939-2946.
12. Yang, Y.B., Ryu, C., Khor, A., Yatesb, N.E., Sharifi, V.N., and Swithenbank, J., *Effect of fuel properties on biomass combustion. Part II. Modelling approach-identification of the controlling factors.* Fuel, 2005. 84(16): p. 2116-2130.
13. Johansson, R., Thunman, H., and Leckner, B., *Sensitivity analysis of a fixed bed combustion model.* Energy and Fuels, 2007. 21: p. 1493-1503.
14. Hicks, R.E., *Pressure Drop in Packed Beds of Spheres.* Industrial & Engineering Chemistry Fundamentals, 1970. 9(3): p. 500-502.
15. Bellais, M., *Modelling of the pyrolysis of large wood particles.* PhD Thesis, KTH - Royal Institute of Technology, Department of Chemical Engineering and Technology, 2007.
16. Peters, B., Schröder, E., Bruch, C., and Nussbaumer, T., *Measurements and particle resolved modelling of heat-up and drying of a packed bed.* Biomass and Bioenergy, 2002. 23(4): p. 291-306.
17. Asthana, A., Menard, Y., Sessiecq, P., and Patisson, F., *Modeling on-grate MSW incineration with experimental validation in a batch Incinerator.* Industrial & Engineering Chemistry Research, 2010. 49(16): p. 7595-7604.
18. Borman, G.L., and Ragland, K. W., *Combustion Engineering, 1st ed.* McGraw-Hill, Boston, ISBN 0-07-006567-5, 1998: p. 363-367.

19. Yang, Y.B., Yamauchi, H., Sharifi. V. N., and Swithenbank, J., *Effects of fuel devolatilisation on the combustion of wood chips and incineration of simulated municipal solid wastes in a packed bed.* Fuel, 2003. 82(18): p. 2205-2221.
20. Yang, Y.B., Newman, R., Sharifi, V. N., Swithenbank, J., Ariss, J., *Mathematical modelling of straw combustion in a 38 MWe power plant furnace and effect of operating conditions.* Fuel, 2007. 86: p. 129-142.
21. Gort, R., *On the propagation of a reaction front in a packed bed: thermal conversion of municipal waste and biomass* PhD Thesis, Universiteit Twente, Enschede, 1995.
22. Klason, T., *Modelling of biomass combustion in furnaces.* PhD Thesis, Lund Institute of Technology, Department of Energy Science, 2006.
23. Klason, T., Bai, X.S., Bahador, M., Nilsson, T.K., and Sunden, B., *Investigation of radiative heat transfer in fixed-bed biomass furnaces.* Fuel, 2008. 87(10): p. 2141-2153.
24. Ahmed, Z.U., *An experimental and numerical study of surface interactions in turbulent swirling jets*. PhD Thesis, Edith Cowan University, School of Engineering, 2016.
25. Moffat, R.J., *Describing the uncertainties in experimental results.* Experimental thermal and fluid science, 1988. 1(1): p. 3-17.
26. Montgomery, D.C. and Runger, G.C., *Applied statistics and probability for engineers*. 5th ed. 2010, USA: John Wiley & Sons. 370-380.
27. *NI 9213 Operating instructions and specifications*, N.I. Corporation, 2009, Austin, USA.
28. *ServoPro Configuration and operation 4000 Series*, S.G. Limited, 2011, East Sussex, UK.